Application of Pullulan as a Standard Polymer for Ionic Liquid Solutions.

胡, 皓

Application of Pullulan as a Standard Polymer for Ionic Liquid Solutions.

（イオン液体溶液用標準高分子試料としてのプルランの適用）

HU HAO
胡　皓
Department of Molecular & Material Sciences
Interdisciplinary Graduate School of Engineering Sciences
Kyushu University

Contents

Chapter 1 Introduction 1

1-1 Insoluble Natural Polymer in Ionic Liquid. 1

1-2 Polymer Solution in Dilute region. 4

1-3 Research Objectives. 12

References 13

Chapter 2 Experiments 19

2-1 Materials. 19

2-2 Sample Preparation 19

2-3 Density Measurement 24

2-4 Rheological Measurements. 24

References 25

Chapter 3 Density for pullulan/ionic liquids solutions 26

3-1 Introduction 26

3-2 Results and Discussion 26

3-3 Summary 34

References 35

Chapter 4 Intrinsic viscosity of pullulan in ionic liquid solutions 36

4-1 Introduction 36

4-2 Results and Discussion 36

4-3 Summary 54

References 54

Chapter 5 Viscoelastic properties of dilute pullulan/ILs solutions 56

5-1 Introduction 56

5-2 Results and Discussion 56

5-3 Summary 84

References 85

Chapter 6 Conclusions 86

Publications 88

Acknowledgment 89

Chapter 1 Introduction

1-1 Insoluble Natural Polymer in Ionic Liquid.

Human being have been utilized natural polymers for a long time. As the representative of them, current situation for cellulose is mainly summarized below. Cellulose is a linear polysaccharide which is most abundant organic compound on the Earth. [1] Due to its renewable and biodegradable properties[2] and also by the processability, cellulose is widely used as a raw material in industrial applications such as textiles, plastics, paper products, coatings, paint, food, and pharmaceutical industries.[3),4)] In the above usage, dissolution of cellulose is important for its processing and chemical derivatization. However, the strong intra- and inter molecular hydrogen bonds between –OH in glucose units[5] interrupt dissolution of cellulose into water and most of conventional solvent systems.[6] Up to date, more than 100 solvent systems have been reported for dissolving cellulose[1] such as N,N-dimethylacetamide/lithium chloride (DMAc/LiCl)[7)~9)], N-methylmorpholine oxide (NMMO)[10], N,N-dimethylformamide/nitrous tetroxide (DMF/N_2O_4)[11], dimethyl sulfoxide (DMSO)/ammonium fluorides[12),13)], and molten salt hydrates, for example, $LiClO_4 \cdot 3H_2O$ and $LiSCN \cdot 2H_2O$[14], However there still suffer drawbacks for these solvents, such as high toxicity, cost, volatility, generation of poisonous gas, difficulty in solvent recovery, or instability in processing.[15]

Ionic liquid (IL) is a generic name of organic salts having low melting point which exists as liquid at around room temperature.[16), 17)] Because of the unique characteristics such as extremely low vapor pressure, thermal stability, and high ionic conductivity, ILs are widely used in many science and engineering fields including synthesis[18), 19)] (organic and inorganic), catalyst[18)], physical chemistry[20), 21)], and advanced materials. [22), 23), 24)]

In 2002 Rogers *et al* [25)] reported that cellulose could be dissolved without derivatization in high concentrations using ionic liquids 1-butyl-3-methylimidazolium chloride (BmimCl) whose melting point is below 100 °C. Following the pioneering work, ILs are widely investigated by many researchers as solvent for insoluble natural polymers. Now, imidazolium-based ionic liquids such as 1-butyl-3 methylimidazolium chloride (BmimCl)[25)], 1-allyl-3-methylimidazolium chloride (AmimCl) [26)], and 1-ethyl-3-methylimidazolium acetate (EmimAc) [27)] have been focused on as new green solvents of cellulose. A several expectations for new processing ways to produce new materials[28), 29)] by using the IL solution of cellulose as well as a few rheological studies of polymers as an attempt for its characterization using ILs as solvents have been reported.[30)~37)] As seen in these foregoing studies of IL solution of cellulose, rheological measurements are more or less utilized to examine processing conditions or attempt to clarify molecular characteristics. Note that most of conventional characterization methods widely used for ordinary polymer-solvent systems, such as

GPC and capillary viscometry, are inadequate for the IL solutions of polymers because of the characteristics of ILs such as high viscosity. Therefore, precise rheological measurements of IL solutions have great importance.

The dissolution of cellulose and other insoluble natural polymers in ILs may give a new opportunity to understand their molecular characteristics and innovations for new processing technology of these natural polymers. However, there are still many issues to be investigated, both in scientific and technological fields, compared to the synthetic polymers. For example the most fundamental issues is why ILs can dissolve those polymers.[38] It is considered that the interactions between the anions of ILs and cellulose play an important role in the solvation[39, 40], while for the role of cations, the detail is not clear.[41 ~ 43] However, this issue is far beyond from the scope of this study. Instead, the molecular characterization of polymers after dissolution into ILs are focused in this study. Note that the degradation of cellulose chains more or less take place during dissolution process.[44, 45]

Studies for standard samples, such as polystyrene with narrow molecular weight distributions (MWD) covering wide range of molecular weight *M* played an important role in the progress in polymer science and industry of synthetic polymers. Both *M* and MWD are important factors for processing and performance of products. Rheological studies are one of major issue linking

molecular characteristics and applications.[46] It is expected that the rheological studies of standard samples in ILs can also contribute for the further advance in studies of natural polymers which can be dissolved into ILs but not into conventional solvents.

Pullulan is a linear polysaccharide polymer consist of α-1,6 linked maltotriose units. Since it is a water soluble polymer and whose properties in aqueous solution are clarified[47) ~ 49)], the series of fractionated samples by molecular weight are used as standard polymer for water soluble polymers. Since pullulan is also soluble into ILs, as reported in this study, it is a candidate of a standard sample for IL soluble polymers. The issues should be studied are summarized in the following subsections.

1-2 Polymer Solution in Dilute region.

In general, polymer solutions can be classified into three regions by using the critical concentration for coil overlapping C^*. [50) ~52)] Here C^* describes concentration in a polymer coil defined by

$$C^* = \frac{M/N_A}{\frac{4}{3}\pi {R_G}^3} \qquad (1)$$

Where R_G is radius of gyration of polymer chain and N_A is Avogadro number. In the dilute region, $C < C^*$, the individual coils are well separated from one another and are almost free to move independently. As C approaches C^*, interactions among chains become stronger and chains start to overlapp with each other at $C = C^*$. The region $C > C^*$ is called semidilute region, in which chains

are overlapped but thermodynamic interactions between part of chains still exist. At $C \gg$ 0.2-0.3 g/cm^3, that is in the concentration region, thermodynamic interaction is shielded by dense segments. Polymer chains entangle with each other when they are long enough so that the molecular motions are sufficiently decreased resulting in high viscosity in semidilute entangled region and concentrated entangled region.

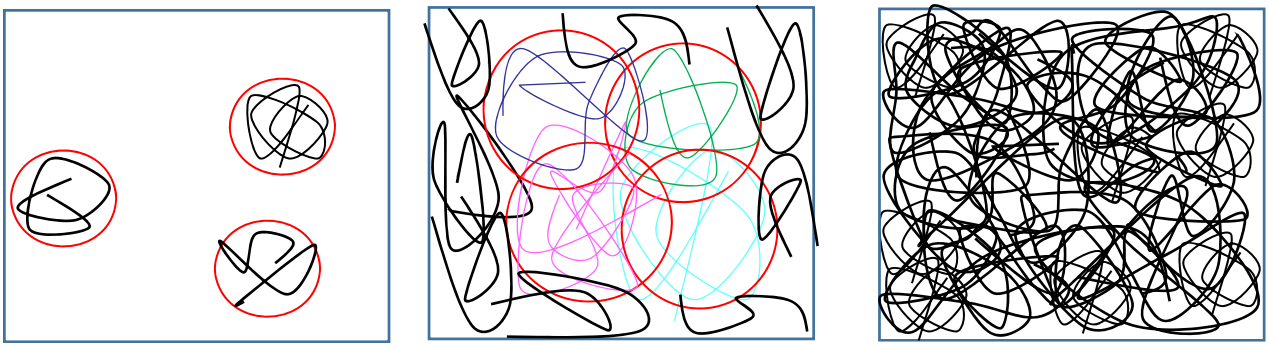

Dilute region $C < C^*$ | Semidilute region $C > C^*$ | Concentrated region $C \gg$ 0.2-0.3 g/cm^3

Figure 1-1. The concentration regions of polymer solution.

The study of dilute polymer solution is most important for understanding the behavior of single polymer chain. The intrinsic viscosity $[\eta]$ is a measure of the hydrodynamic size of polymer coil in the dilute solution.[53] It can be determined from measurements of solvent viscosity η_s and zero shear viscosity η^0 of solutions. The relative viscosity η_{rel} ($=\eta^0/\eta_s$) and specific viscosity η_{sp} ($=\eta_{rel}$-1) are obtained and by using the plots of η_{sp}/C and $\ln\eta_{rel}/C$ vs C, $[\eta]$ is determined as a value extrapolated

to the zero concentration limit.[54] In the dilute solutions the relationship $R_G \propto M^v$ can be obtained, as v = 0.5 for theta solvent (Gaussian chain), and v = 0.6 for expanded chain due to excluded volume effect in good solvents.[55] By the Flory-Fox viscosity equation, $[\eta]$ can be described by R_G and M as

$$[\eta] = \emptyset \frac{<R_G{}^2>^{\frac{3}{2}}}{M} \quad (2)$$

Where $\emptyset$ is Flory viscosity factor. Furthermore, another relationship of $[\eta]$ and molecular weight M for polymer can be represented as equation 3, which is called Mark-Houwink-Sakurada (MHS) equation, in which α range from 0.5 to 0.8 for the most flexible polymers. A value of 0.5 is indicative of a theta solvent, while 0.8 is a limiting value for good solvents.[53]

$$[\eta] = KM^{\alpha} \quad (3)$$

Therefore the relationship between $[\eta]$ and M can be expressed as $[\eta] \propto M^{\alpha} \propto M^{3v-1}$. According to the equation 1, the relationship between C^* and $[\eta]$ can be obtained as $C^* \simeq 1 / [\eta]$.

The polymer concentration C and molecular weight dependence of the zero-shear viscosity η^0 of linear polymer solutions over a wide range of polymer concentration have been studied well for many polymer solvent systems.[46), 56), 57)] The reported equations can be used to estimate M when MWD is relatively narrow; M obtained from $[\eta]$ by using equation 3 is close to weight-averaged one,

M_w. In the dilute region, the zero shear viscosity η^0 can be expressed by the expansion form of $C[\eta]$ as equation 4, where η_R^0 is the reduced specific viscosity, $\eta_R^0 = \eta_{sp} / C[\eta]$ and k' is Huggins constant.

$$\eta_R^0 \equiv \eta_{sp} / C[\eta] = 1 + k'[\eta]C + \ldots \qquad (4)$$

It has been reported that for the linear polymer in good solvent k' is around 0.35.[57), 58)]

Viscoelastic properties of linear flexible polymers in dilute solutions in Θ solvents are theoretically discussed by Rouse and Zimm using the bead-spring model.[46)] In this model, a polymer chain is constructed using N beads and N – 1 spring units as shown in Figure 1-2. This chain preserves Gaussian nature of polymer chain, spring unit is equivalent to statistical segment. Rouse theory describes free draining Gaussian chains by neglecting hydrodynamic interactions between beads.[60)] Zimm theory describes the behavior with strong hydrodynamic interaction (non-draining limit).[61)]

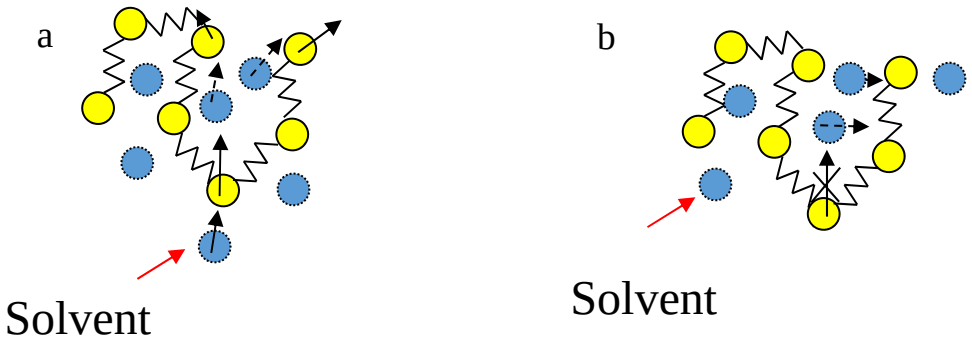

Figure 1-2. Bead-spring model of Zimm (a) and Rouse (b) theory.

According to the Rouse-Zimm (RZ) theory, the storage modulus G' and the loss modulus G'' can be expressed as the following general formulae,

$$G''(\omega) = \frac{CRT}{M}\sum_{p=1}^{N}\frac{\omega\ \tau_P}{1+\omega^2{\tau_P}^2} + G''(solvent) \qquad (5)$$

$$G'(\omega) = \frac{CRT}{M}\sum_{p=1}^{N}\frac{\omega^2{\tau_P}^2}{1+\omega^2{\tau_P}^2} \qquad (6)$$

$$G''(solvent\ ) = \omega\eta_s \qquad (7)$$

$$\tau_p = \frac{\tau_{RZ}}{p^{\alpha}} \qquad (8)$$

where C is the polymer concentration, R is the gas constant, T is the temperature, M is the molecular weight, and ω the angular frequency. Usually G'' (solvent) $=\omega\eta_s$, η_s being solvent viscosity. τ_p is the relaxation time of p-th normal mode defined in eq. (8) and τ_{RZ} is the longest relaxation time, which can be determined from the terminal region data. The parameter α denotes strength of the hydrodynamic interaction: $\alpha = 2$ corresponds to free-draining limit, while $\alpha = 1.5$ corresponds to non-draining limit.[55] Equation 9 provides another method to determine τ_p by using the zero shear viscosity η^0 of solutions for the Rouse model when η_s is negligible. In this case, p = 1 corresponds to the longest relaxation time.

$$\tau_p = \frac{6\eta_0 M}{\pi^2 p^2 CRT} \qquad (9)$$

It is predicted from Zimm and Rouse theories that the viscoelastic properties of linear polymers at infinite dilution [G'] and [G''] in the higher ω region are different as shown in Figure 1-3.

It should be emphasized again that original RZ theories argue Gaussian chains at infinite dilution. However, it is widely accepted that the Rouse model can well explain the linear viscoelastic properties of non-entangled melts (by replacing C with density ρ) over a wide range of ω.[62), 63)] Note that the remaining contributions from glassy zone G^*_G (relaxation of glass modulus) in dynamic moduli G^* cannot be always neglected when measuring temperature is not far from glass transition temperature T_g.[62)] It is also true in solutions when glass forming solvents are used.[64)] For non-entangled solutions at finite C, it is also known that behaviors of G^* alter from Zimm-like to Rouse-like with increase of C. Efforts has been made to fit experimental data with RZ theory by adjusting parameters therein.[65), 66)] However, the deviation of measured data from RZ calculations are apparent for G' in the terminal region.

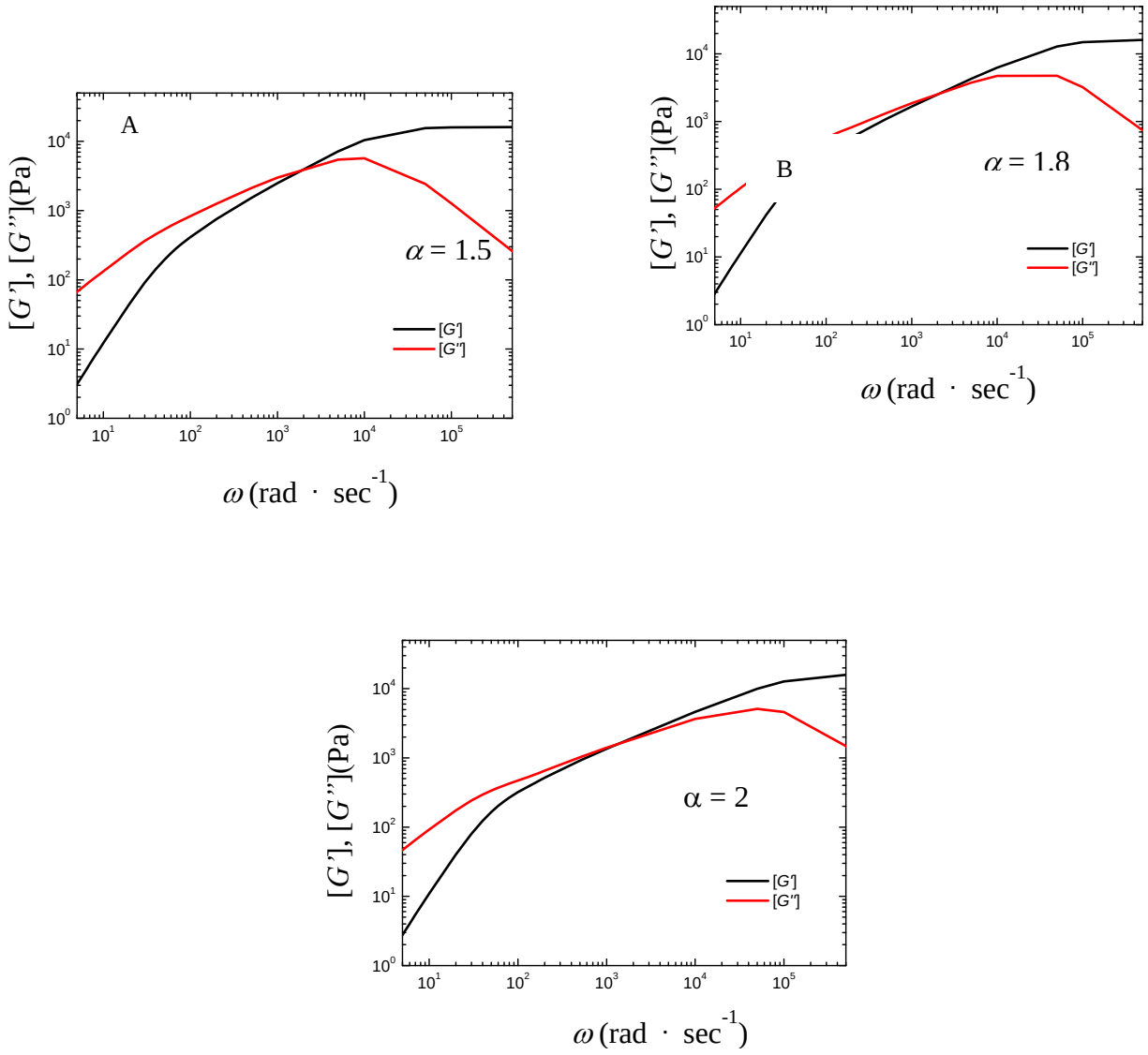

Figure 1-3. Double logarithmic plots of G' and G'' vs ω for Rouse-Zimm model with different parameter α.

Osaki *et al*.[67] systematically studied G^* data for standard polystyrene in a good solvent and employed correction term called long-time (LT) term to get a good fit at low ω;

$$G'_{LT} = G_{LT}\frac{\tau_{LT}{}^2\omega^2}{1+\tau_{LT}{}^2\omega^2} \qquad (10)$$

$$G''_{LT} = G_{LT}\frac{\tau_{LT}\omega}{1+\tau_{LT}{}^2\omega^2} \qquad (11)$$

$$G_{LT} = QC[\eta]\frac{CRT}{M} \qquad (12)$$

$$\tau_{LT} = P\tau_{RZ} \qquad (13)$$

where Q and P being adjustable parameters (Q = 0.09 and P = 5 in their study). The calculated G" with and without LT term are practically the same, while G' data in the lower frequency region can be well fitted by addition of the LT term as,

$$G'(\omega) = \frac{CRT}{M}\sum_{p=1}^{N}\frac{\omega^2\tau_P{}^2}{1+\omega^2\tau_P{}^2} + G_{LT}\frac{\tau_{LT}{}^2\omega^2}{1+\tau_{LT}{}^2\omega^2} \qquad (14)$$

The LT term is related to the hydrodynamic radius of polymer chain at infinite dilution through intrinsic viscosity $[\eta]$. Change in the excluded volume effect and hydrodynamic interaction with increase of C are expressed as a function of degree of coil overlapping C/C^* ~ $C[\eta]$. In their discussion, chain overlapping concentration C^* is chosen as $C^* = 2.5/[\eta]$ based on the Einstein's viscosity equation.[68] Note that this threshold is in good agreement with the transition from dilute to

(non-entangled) semidilute region discussed for thermodynamic properties such as osmotic pressure and correlation length.[52)]

1-3 Research Objectives.

As mentioned in section 1.2, the rheological properties of synthetic linear polymers are well investigated by using standard polymers. However, the general behaviors observed for standard polymers are limited to linear flexible polymers in non-ionic solvents.[46)] The behaviors of polymers with electrostatic interactions are different as studied for polyelectrolytes.[69) ~71)] To develop the study for insoluble natural polymer in ILs, therefore, standard natural polymer in IL solutions have to be investigated to test the applicability of knowledge for standard polymers in ordinary solvents.

In this study, viscoelastic properties of standard pullulan samples with different molecular weights and narrow MWD in BmimCl, AmimCl, and EmimAc are studied in comparison with the behaviors of standard linear polystyrenes in dilute solutions. The following part of this thesis is structured as follows:

The experiments in this thesis are summarized in section 2. In section 3, the density of pullulan/ionic liquids solutions are studied at different temperatures. Empirical relationships between density ρ and wt% concentration c of pullulan in ILs are established. In section 4, intrinsic viscosity of pullulan in ILs are discussed. In section 5, the viscoelastic properties of pullulan in ILs are studied

by using Rouse-Zimm model, comparing to the results for synthetic linear polymers. An application for determining the M_w of insoluble natural polymer by using Rouse-Zimm model fitting is also discussed. At last, section 6 is the conclusion of this thesis.

Reference.

1) Cellolose Gakkai, Ed. "*Cellulose no giten*", (2000), Asakura Syoten, Tokyo.

2) Tsioptsias C, Stefopoulos A, Kokkinomalis I, Papadopoulou L, and Panayiotou C, *Green Chem*., **10**, 965‐971, (2008).

3) Edgar KJ, Buchanan CM, Debenham JS, Rundquist PA, Seiler BD, Shelton MC, and Tindall D, *Prog. Polym. Sci.*, **26**, 1605‐1688, (2001).

4) Richardson S, Gorton L, *Anal. Chim. Acta,* **497**, 27, (2003).

5) Updegraff DM, *Anal. Biochem.*, **32**, 420‐424, (1969).

6) Ohno H, and Fukaya Y, *Chem. Lett.*, **38**, 2‐7, (2009).

7) McCormick CL, Callais PA, Hutchinson BH Jr, *Macromolecules,* **18**, 2394–2401, (1985).

8) McCormick CL, and Dawsey TR, *Macromolecules*, **23**, 3606‐3610, (1990).

9) Matsumoto T, Tatsumi D, Tamai N, Takaki T, *Cellulose,* **8**, 275–282, (2001).

10) Fink HP, Weigel P, Purz HJ, Ganster J, *Prog. Polym. Sci.,* **26**, 1473–1524, (2001).

11) Hammer RB, and Turbak AF, *Abstracts of Papers of the American Chemical Society*, **173**, 8‑8, (1977).

12) Ciacco GT, Liebert TF, Frollini E, and Heinze TJ, *Cellulose*, **10**, 125‑132, (2003).

13) Ramos LA, Frollini E, Heinze T, *Carbohydr. Polym.,* **60**, 259–267, (2005).

14) Fischer S, Leipner H, Thu¨mmler K, Brendler B, Peters J, *Cellulose* **10**, 227–236, (2003).

15) Rosenau T, Potthast A, Sixta H, and Kosma P, *Prog. Polym. Sci*., **26**, 1763‑1837, (2001).

16) Ohno H, *"Ionic liquids: The Front and Future of Material Development"*, (2006), CMC Shuppan, Tokyo.

17) Rogers RD and Seddon KR, Science, **302**, 792‑793, (2003).

18) Welton T, *Chem. Rev.* **99**, 2071-2083, (1999).

19) Kubisa P, *J. Polym. Sci. Part A: Polym. Chem.* **43**, 4675–4683, (2005).

20) Seddon KR, Stark A, Torres MJ, *Pure. Appl. Chem.***72**, 2275-2287, (2000).

21) Yang Q, Zhang H, Su B, Yang Y, Ren Q, and Xing H, *J. Chem. Eng. Data,* **55***,* 1750–1754, (2010).

22) Poplin JH, Swatloski RP, Holbrey JD, Spear SK, Metlen A, Gratzel M, Nazeeruddin MK, Rogers RD, *Chem. Commun* (UK). **20**, 2025, (2007).

23) Wu J, Zhang J, Zhang H, He J, Ren Q, Guo M, *Biomacromolecules.* **5**, 266–268, (2005).

24) Lu J, Yan F, Texter J, *Prog. Polym. Sci.* **34**, 431, (2009).

25) Swatloski RP, Spear SK, Holbrey JD, Rogers RD, *J. Am. Chem. Soc.* **124**, 4974-4975, (2002).

26) Zhang H, Wu J, Zhang J, He J, *Macromolecules,* **38**, 8272–8277 (2005).

27) Kosan B, Michels C, Meister F, *Cellulose,* **15**, 59-66 (2008).

28) Turner MB, Spear SK, Holbrey JD, Rogers RD, *Biomacromolecules*, **5**, 1379, (2004).

29) Shang S, Zhu L, Fan J, *Carbohydrate Polymers*, **86**, 462-468, (2011).

30) Sammons RJ, Collier JR, Rials TG, Petrovan S, *J. Appl. Polym. Sci,* **110(2)**, 1175-1181, (2008).

31) Collier JR, Watson JL, Collier BJ, Petrovan S, *J. Appl. Polym. Sci,* **111(2)**, 1019-1027, (2009).

32) Maeda A, Inoue T, Sato T, *Macromolecules*, **46**, 7118, (2013).

33) Kuang QL, Zhao JC, Niu YH, Zhang J, Wang ZG, *J. Phys. Chem. B*, **112**, 10234-10240, (2008).

34) Chen X, Zhang Y, Cheng LY, Wang HP, *J. Polym. Environ*, **17**, 273-279, (2009).

35) Chen X, Zhang Y, Wang H, Wang SW, Liang S, and Colby RH, *J. Rheol.*, **55**, 485, (2011).

36) Kosan B, Schwikal K, Meister F, *Cellulose*, **17**, 495-506, (2010).

37) Gericke M, Schlufter K, Liebert T, Heinze T, and Budtova T, *Biomacromolecules*, **10**, 1188-1194, (2009).

38) Wang H, Gurau G, and Rogers RD, *Chem. Soc. Rev.*, **41**, 1519–1537, (2012).

39) Xu AR, Wang JJ, and Wang HY, *Green Chem.*, **12**, 268‑275, (2010).

40) Fukaya Y, Hayashi K, Wada M, and Ohno H, *Green Chem*., **10**, 44‑46, (2008).

41) Remsing RC, Swatloski RP, Rogers RD, and Moyna G, *Chem. Commun*., 1271‑1273, (2006).

42) Novoselov NP, Sashina ES, Petrenko VE, and Zaborsky M, *Fibre Chem.*, **39**, 153‑158, (2007).

43) Zhang JM, Zhang H, Wu J, Zhang J, He JS, and Xiang JF, *Phys. Chem. Chem. Phys*., **12**, 1941‑1947, (2010).

44) Heinze T, Schwikal K, and Barthel S, *Macromol. Biosci*., **5**, 520-525, (2005).

45) Vitz J, Erdmenger T, Haensch C, and Schubert US, *Green Chem.,* **11**, 417-424, (2009).

46) Ferry JD, "*Viscoelastic Properties of Polymers*", 3rd ed, (1980), John Wile & Sons Inc, NY.

47) Kato T, Okamoto T, Tokuya T, Takahashi A, *Biopolymers*, **21**, 1623-1633, (1982).

48) Kawahara K, Ohta K, Miyamoto H, Nakamura S, *Carbohydr. Polym*, **4**, 335-356, (1984).

49) Nishinari K, Kohyama K, Williams PA, Phillips GO, Burchard W, and Ogino K, *Macromolecules*, **24**, 5590-5593, (1991).

50) Noda I, Kato N, Kitano T, Nagasawa M, *Macromolecules*, **14**, 668, (1981).

51) Higo Y, Ueno N, Noda I, *Polym. J*. **15**, 367, (1983).

52) Noda I, Higo Y, Ueno N, Fujimoto T, *Macromolecules*, **17**, 1055, (1984).

53) Lapasin R, Pricl S, "*Rheology of industrial polysaccharides: theory and applications"* (1995). Blackie Academic and Professional, Glasgow.

54) Huggins ML, *J. Am. Chem. Soc*, **64**, 2716–2718, (1942).

55) Doi M, Edwards SF, "*The Theory of Polymer Dynamics"* (1986). Oxford University Press, Oxford.

56) Berry GC, Fox TG, *Adv. Polym. Sci.*, **5**, (1968).

57) Graessley WW, *Adv. Polym. Sci.*, **16**, (1974).

58) Takahashi Y, Isono Y, Noda I, Nagasawa M, *Macromolecules*, **18***,* 1002-1008, (1985).

59) Takahashi Y, Sakakyra D, Wakutsu M, Yamaguchi M, Noda I, *Polymer Journal*, **24**, 9, 987-990, (1992).

60) Rouse PE, *J Chem Phys,* **21**, 1272, (1953).

61) Zimm BH, *J Chem Phys,* **24**, 269, (1956).

62) Ferry JD, Landel RF, and Williams ML *Journal of Applied Physics,* **26**, 359, (1955).

63) Onogi S, Masuda T, Kitagawa K, *Macromolecules*, **3**,109-116, (1970).

64) Morishima K, Inoue T, *Journal of the Society of Rheology, Japan (Nihon Reoroji Gakkaishi)* **41**, 151-156, (2012).

65) Hair DW, Amis EJ, *Macromolecules*, **22**, 4528-4536, (1989).

66) Colby RH, *Rheol,* **49**, 25–442, (2010).

67) Osaki K, Inoue T, Uematsu T, *Journa of Polymer Science: Part B: Polymer Physics,* **39**, 211–217, (2001).

68) Osaki K, Inoue T, Uematsu T, Yamashita Y, *Journa of Polymer Science: Part B: Polymer Physics,* **40**, 1038–1045, (2002).

69) Yamaguchi M, Yamaguchi Y, Matsushita Y, and Noda I, *Polym. J.*, **22**, 1077, (1990).

70) Yamaguchi M, Wakutsu M, Takahashi Y, and Noda I, *Macromolecules*, **25**, 470-474, (1992).

71) Yamaguchi M, Wakutsu M, Takahashi Y, and Noda I, *Macromolecules*, **25**, 475-478, (1992).

Chapter 2 Experiments

2-1 Materials.

EmimAc (purity: 97%, water content: ≦0.5%) was purchased from Sigma-Aldrich and used as received. BmimCl and AmimCl was synthesized and purified following the method in literatures with slight modification.[1) ~ 3)] Toluene was used as solvent in our synthesis. Pullulan sample for density measurement (about 100 kg/mol) was used as received from Hayashibara Co., Ltd. The standard pullulan samples with different molecular weights and narrow MWDs are purchased from Showa Denko K. K. and used without further purification. Weight averaged molecular weight M_w and MWD index M_w/M_n, where M_n is number averaged molecular weight, are tabulated in Table 1. Before the preparation of the solutions, all the pullulan samples and ILs were dried *in vacuo* at 60°C for 12 hrs.

2-2 Sample Preparation.

According to a preliminary study[4)], homogeneous pullulan/BmimCl solution cannot be prepared at temperatures lower than 80°C. On the other hand, when the temperature was raised higher than

80°C, degradation and oxidation of pullulan was confirmed by intrinsic viscosity measurement for aqueous solution of pullulan recovered from the BmimCl solution as shown in Figure 2-1. Therefore, pullulan solution in BmimCl is prepared by the following method. First aqueous solution of pullulan was prepared and then mixed with prescribed amount of BmimCl. Next, the sample solution was dried at 60°C *in vacuo* to remove the water for 72hrs. By the same method pullulan/AmimCl solutions are also prepared. The water content of sample solutions were measured by Karl-Fischer titration method and confirmed that it is always less than 2 wt% for BmimCl solutions and less than 1.5 wt% for AmimCl solutions. EmimAc solutions of pullulan were directly prepared by dissolution of pullulan into EmimAc at 60°C *in vacuo* for 72hrs. The solutions were clear and the water content were less than 1 wt%. Intrinsic viscosities [η] for pullulan in aqueous solution for recovered samples from BmimCl and from EmimAc are 106.9 cm^3/g and 105.1 cm^3/g, respectively as shown in Figure 2-2, Figure 2-3. Both are reasonably close to the value 105.3 cm^3/g for the fresh sample, confirming that no sample degradation occurred by the above protocol.

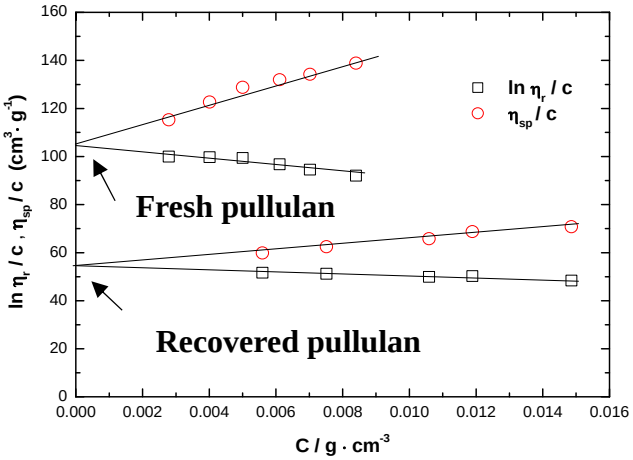

Figure 2-1. Comparison of intrinsic viscosities [η] for pullulan in aqueous solution for fresh and recovered samples which was prepared at 80°C with [η] of fresh samples.

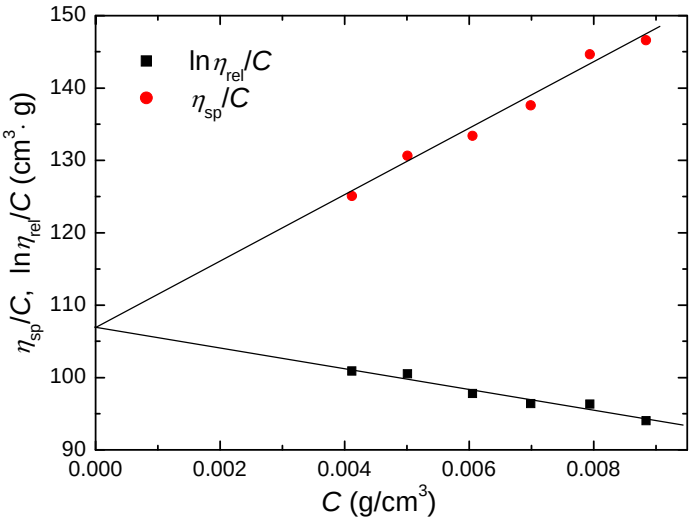

Figure 2-2. Intrinsic viscosity [η] for pullulan in aqueous solution for recovered sample which was prepared at 60°C in BmimCl.

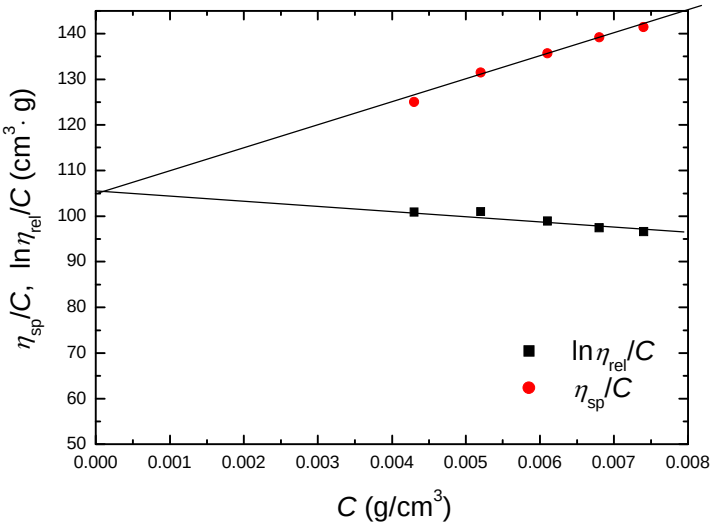

Figure 2-3. Intrinsic viscositiy [η] for pullulan in aqueous solution for recovered samples which was prepared at 60°C in EmimAc.

Table I Molecular characteristics of pullulan samples

Sample codes	M_w [(a)]	M_w/M_n [(b)]
Lot 5H23	around 100k	unknown
P-1300	1.33×10^6	1.37
P-800	7.88×10^5	1.23
P-400	3.93×10^5	1.10
P-200	2.12×10^5	1.13
P-100	1.13×10^5	1.13
P-50	4.88×10^4	1.07
P-20	2.28×10^4	1.07
P-10	1.18×10^4	1.10
P-5	0.59×10^4	1.09

(a): M_w determined by ultra-centrifugal sedimentation equilibrium, reported by manufacture.

(b): M_w/M_n determined by size exclusion chromatography, reported by manufacture.

2-3 Density Measurement.

The density ρ (g/cm^3) of pullulan solutions on BmimCl, AmimCl and EmimAc at different concentrations were measured at atmospheric pressure in a DMA 4500 Anton Parr density meter at different temperatures ranging from 10.00 °C to 80.00 °C. Temperature were controlled within ± 0.05 °C at each measurement. The uncertainty of the measurements was estimated to be better than ± 1×10^{-4} g/cm^{-3}.

2-4 Rheological Measurements.

Rheological measurements are carried out in an MCR-300 rheometer (Anton Paar GmbH) equipped with peltier temperature control system with 50 mmϕ and 1° cone-plate geometry under N_2 atmosphere. To prevent moisture adsorption during sample loading and to reduce the contamination of air during measurements, a homemade plastic chamber surrounding the original sample chamber filled with N_2 gas was used. N_2 gas was supplied from ordinary cylinder (dew point *ca* -50 °C). Both oscillatory and steady shear measurements are carried out for solutions and solvents in a temperature (T) range from 10 to 40 °C, mainly at 25 °C. Dynamic oscillatory shear measurement are carried out in a frequency (ω) range from 0.1 to 100 rad/s with varying strain from 5 % to 10 % to maintain linear region measurement.

After the rheological measurements, pullulan samples are recovered from BmimCl and EmimAc

solutions by precipitation method. Intrinsic viscosities of recovered pullulan in aqueous solution was always practically the same with a value for the fresh sample, confirming that no sample degradation occurred by the experiments.

2-5 Reference.

1) *Ion Ekitai (Ionic liquids)* Ⅱ; Ohno, H., ED.;CMC Shuppan: Tokyo, (2006**).**

2) Yamamuro O, Minamimoto Y, Inamura Y, Hayashi S, Hamaguchi H, *Chem. Phys. Lett.* **423**, 371, (2006).

3) Zhang H, Wu J, Zhang J, He J, *Macromolecules,* **38**, 8272–8277, (2005).

4) Kamo M, *Solution property of pullulan ionic liquid solution. Master thesis*.; Department of Molecular & Material Sciences, IGSES, Kyushu University (2009).

Chapter 3 Density for pullulan/ionic liquids solutions

3-1 Introduction.

For precise study of solution properties of polymers, it is essential to establish empirical relationship between concentration of the solution in wt% and in g/cm^3.[1)] Note that ILs are glass forming liquids so that the density may have steep temperature dependence than conventional solvents.[2), 3)] The densities of polysaccharides are higher than synthetic polymers.[4)] Therefore, it should not be assumed to be 1 g/cm^3, as seen in many resent studies for polymer solutions. In this study, the densities of sample solutions up to *ca* 16 wt% are reported. To take into account of effects of remaining water[5) ~ 7)] in ILs and moisture adsorption by ILs, the water content dependence of the density is also examined.

3-2 Result and discussion.

3-2-1 Density of pullulan/ILs solutions.

The values of density ρ for the pullulan/ILs solutions are tabulated in Table 3-1, 3-2 and 3-3. Figure 3-1a, b, c, and Figure 3-2a, b, c show the wt% concentration c and the temperature T dependences of ρ for pullulan/ILs, respectively. It is observed in both solutions that ρ linearly increase with the increase of c and decrease of T. From these results an empirical relationship of

density and concentration can be obtained as,

$$\rho = \alpha c + \rho_0 \qquad (g/cm^3) \qquad (15)$$

where ρ_0 is the density of pure IL. For the pullulan/ILs solutions, the value of α are tabulated in Table 3-4. The uncertainty of α was estimated to be ± 2 × 10^{-5} for pullulan/BmimCl, ±8 × 10^{-5} for pullulan/EMimAc solution and ±6 × 10^{-5} for pullulan/AmimCl solution. By using the equation 15, the density of the pullulan/ILs solutions in any concentration in this range can be determined. Furthermore, the concentration *C* in g/cm^3 can be obtained as

$$C = \rho c/100 \quad (g/cm^3) \qquad (16)$$

For the temperature dependence of density, it is complicated to discuss it near the glass transition temperature. However, at the *T* range from 10.00 °C to 80.00 °C, we obtained

$$\rho = bT + K \qquad (g/cm^3) \qquad (17)$$

where *K* is the value of density at 0 °C, and the value of *b* for several concentrations are tabulated in Table 3-5. The uncertainty of *b* was estimated to be ± 5 × 10^{-6} for all solutions.

Table 3-1. Density ρ of pullulan/BmimCl solution from T = 10 °C to T = 80 °C

	ρ g/cm^3								
c (wt%)	10.00 °C	25.00 °C	30.00 °C	35.00 °C	40.00 °C	50.00 °C	60.00 °C	70.00 °C	80.00 °C
0.00	1.0923	1.0836	1.0807	1.0778	1.0747	1.0687	1.0631	1.0575	1.0520
0.55	1.0942	1.0855	1.0826	1.0796	1.0764	1.0707	1.0651	1.0595	1.0540
1.01	1.0958	1.0871	1.0841	1.0811	1.0779	1.0723	1.0668	1.0612	1.0557
2.26	1.0999	1.0912	1.0882	1.0852	1.0820	1.0764	1.0709	1.0654	1.0599
4.02	1.1052	1.0965	1.0936	1.0907	1.0876	1.0818	1.0762	1.0707	1.0652
5.71	1.1107	1.1021	1.0992	1.0963	1.0934	1.0873	1.0818	1.0763	1.0708
9.77	1.1239	1.1153	1.1124	1.1096	1.1067	1.1009	1.0949	1.0894	1.0839
16.22	1.1453	1.1368	1.1339	1.1311	1.1283	1.1226	1.1170	1.1112	1.1054

Table 3-2. Density ρ of pullulan/EmimAc solution from T = 10 °C to T = 80 °C

	ρ g/cm^3								
c (wt%)	10.00 °C	25.00 °C	30.00 °C	35.00 °C	40.00 °C	50.00 °C	60.00 °C	70.00 °C	80.00 °C
0.00	1.1087	1.0994	1.0964	1.0934	1.0903	1.0843	1.0783	1.0724	1.0665
0.54	1.1095	1.1001	1.0971	1.0941	1.0911	1.0851	1.0791	1.0732	1.0673
0.97	1.1107	1.1013	1.0983	1.0953	1.0923	1.0863	1.0803	1.0744	1.0685
1.65	1.1124	1.1031	1.1000	1.0969	1.0939	1.0880	1.0820	1.0761	1.0702
3.05	1.1171	1.1079	1.1048	1.1018	1.0987	1.0926	1.0866	1.0808	1.0749
4.85	1.1255	1.1163	1.1132	1.1102	1.1072	1.1012	1.0952	1.0892	1.0833
7.13	1.1346	1.1248	1.1218	1.1188	1.1158	1.1098	1.1038	1.0979	1.0920
9.70	1.1404	1.1305	1.1274	1.1244	1.1214	1.1154	1.1095	1.1036	1.0977
16.50	1.1648	1.1556	1.1525	1.1495	1.1464	1.1402	1.1330	1.1281	1.1222

Table 3-3. Density ρ of pullulan/AmimCl solution from T = 10 °C to T = 80 °C

	ρ g/cm^3								
c (wt%)	10.00 °C	25.00 °C	30.00 °C	35.00 °C	40.00 °C	50.00 °C	60.00 °C	70.00 °C	80.00 °C
0.00	1.1537	1.1441	1.1411	1.1382	1.1353	1.1294	1.1238	1.1183	1.1127
0.45	1.1582	1.1488	1.1457	1.1428	1.1399	1.1341	1.1284	1.1228	1.1173
1.21	1.1596	1.1502	1.1471	1.1442	1.1414	1.1356	1.1299	1.1242	1.1187
2.69	1.1640	1.1549	1.1516	1.1486	1.1457	1.1400	1.1343	1.1287	1.1230
6.52	1.1742	1.1651	1.1619	1.1589	1.1560	1.1503	1.1447	1.1391	1.1335
9.08	1.1819	1.1730	1.1710	1.1669	1.1637	1.1579	1.1523	1.1467	1.1411

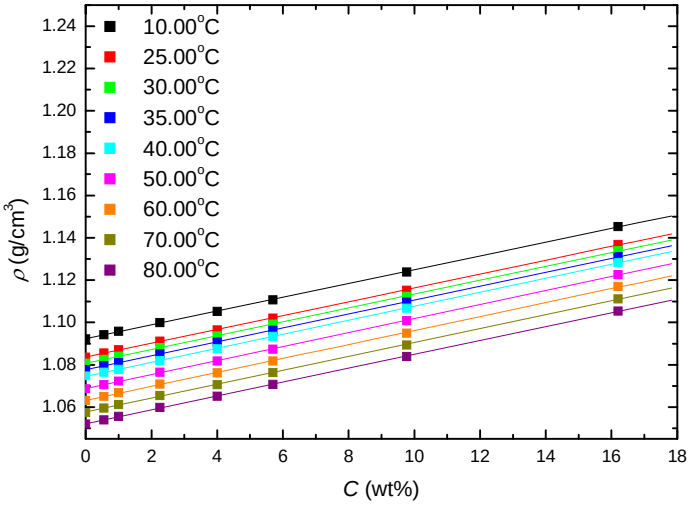

Figure 3-1a. Concentration dependence of the density for pullulan/BmimCl solution at different temperatures.

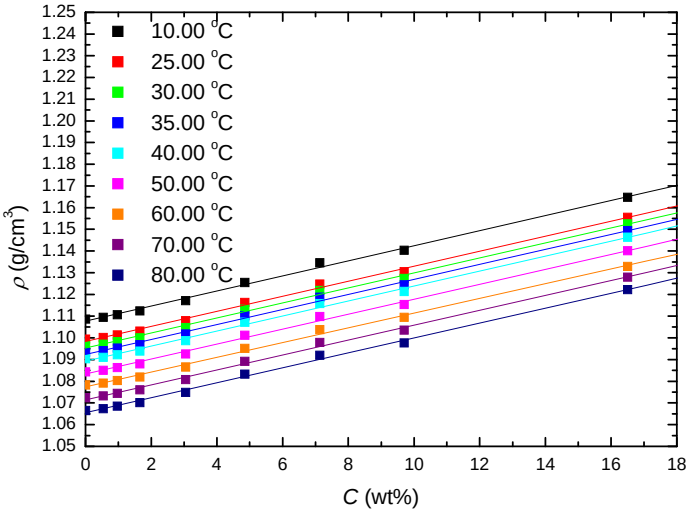

Figure 3-1b. Concentration dependence of the density for pullulan/EmimAc solution at different temperatures.

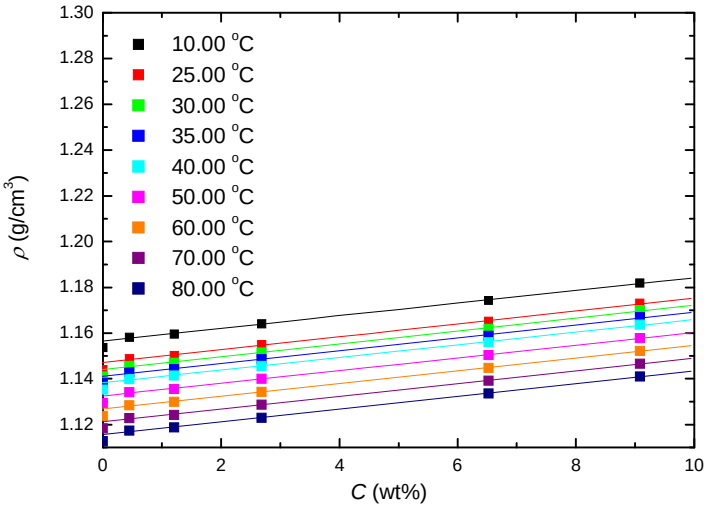

Figure 3-1c. Concentration dependence of the density for pullulan/AmimCl solution at different temperatures.

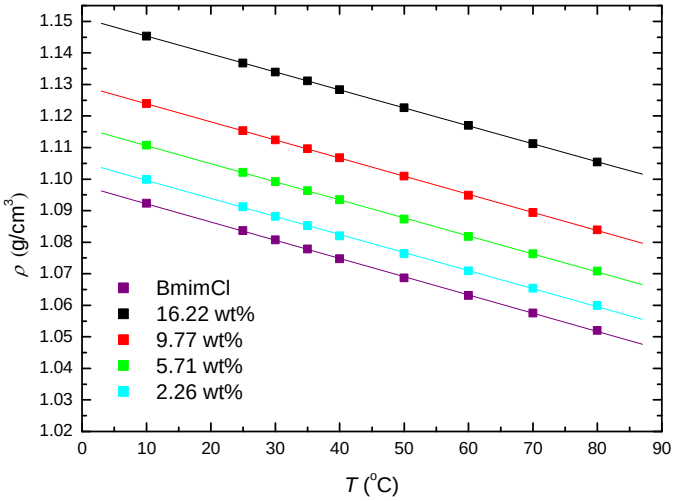

Figure 3-2a. Temperature dependence of the density for pullulan/BmimCl solution at different concentrations.

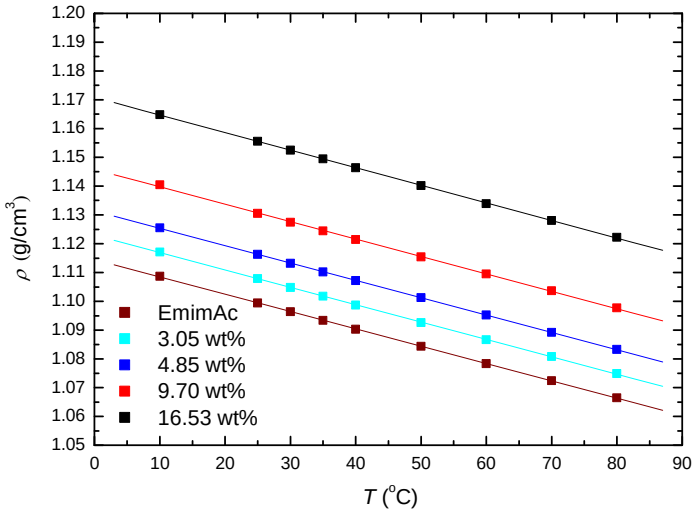

Figure 3-2b. Temperature dependence of the density for pullulan/EmimAc solution at different concentrations.

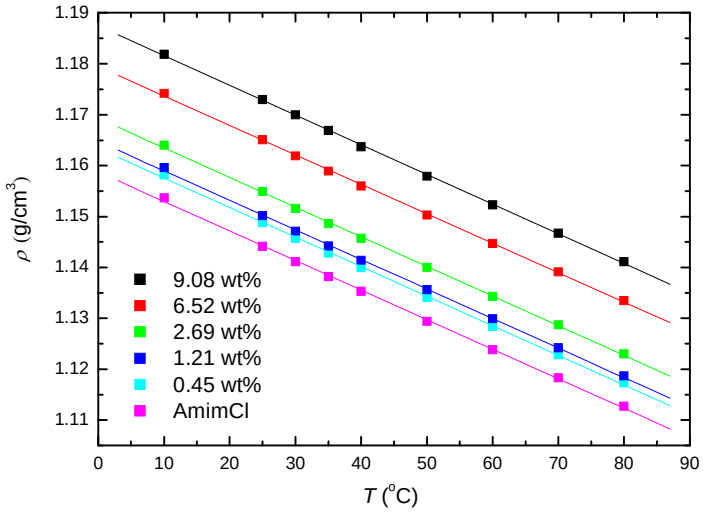

Figure 3-2c. Temperature dependence of the density for pullulan/AmimCl solution at different concentrations.

Table 3-4. Prefactor α in eq. (1) for the pullulan/ILs solution from T = 10.00 °C to T = 80.00 °C

	α		
T	Pullulan/BmimCl	Pullulan/EmimAc	Pullulan/AmimCl
10.00 °C	3.25×10^{-3}	3.47×10^{-3}	2.76×10^{-3}
25.00 °C	3.27×10^{-3}	3.46×10^{-3}	2.81×10^{-3}
30.00 °C	3.27×10^{-3}	3.46×10^{-3}	2.82×10^{-3}
35.00 °C	3.28×10^{-3}	3.46×10^{-3}	2.80×10^{-3}
40.00 °C	3.31×10^{-3}	3.46×10^{-3}	2.77×10^{-3}
50.00 °C	3.31×10^{-3}	3.45×10^{-3}	2.77×10^{-3}
60.00 °C	3.30×10^{-3}	3.39×10^{-3}	2.78×10^{-3}
70.00 °C	3.29×10^{-3}	3.44×10^{-3}	2.79×10^{-3}
80.00 °C	3.27×10^{-3}	3.44×10^{-3}	2.78×10^{-3}

Table 3-5. Prefactor *b* in eq. (3) for the pullulan/ILs solution for several concentrations.

Pullulan/BmimCl		Pullulan/EmimAc		Pullulan/AmimCl	
c	*b*	*c*	*b*	*c*	*b*
0.00 wt%	-5.78×10^{-4}	0.00 wt%	-6.02×10^{-4}	0.00 wt%	-5.81×10^{-4}
2.26 wt%	-5.72×10^{-4}	3.05 wt%	-6.03×10^{-4}	1.21 wt%	-5.81×10^{-4}
5.71 wt%	-5.72×10^{-4}	4.85 wt%	-6.02×10^{-4}	2.69 wt%	-5.83×10^{-4}
9.77 wt%	-5.74×10^{-4}	9.70 wt%	-6.05×10^{-4}	6.52 wt%	-5.78×10^{-4}
16.22 wt%	-5.69×10^{-4}	16.53 wt%	-6.11×10^{-4}	9.08 wt%	-5.84×10^{-4}

3-2-2 Influence of water content for pullulan/ILs solutions.

Since ILs easily absorb moisture, the influence of water content on ρ are also discussed. The density influence of water content C_w in wt% for pullulan/Ils solution are shown in Figures 3-3a and

3-3b. For the pullulan/BmimCl solution, water almost has no influence to the density of the solution with C_w up to 6.6 wt%. Since C_w for all the pullulan/BmimCl solution in this study are lower than 2 wt%, it can be considered that water content has no influence to the density of pullulan/BmimCl solution. The similar result are also obtained for pullulan/AmimCl solutions.

For the pullulan/EmimAc solution, it is observed that density of the solution increases with increasing C_w. In this study, however, C_w in pullulan/EmimAc solutions are lower than 1 wt% so that the influence of water content is also negligible.

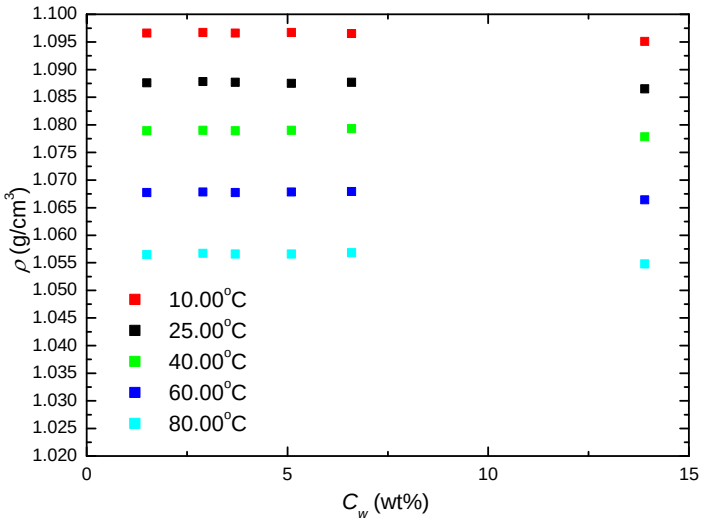

Figure 3-3a. Water content C_w dependence of the density for pullulan/BmimCl solution at different temperatures.

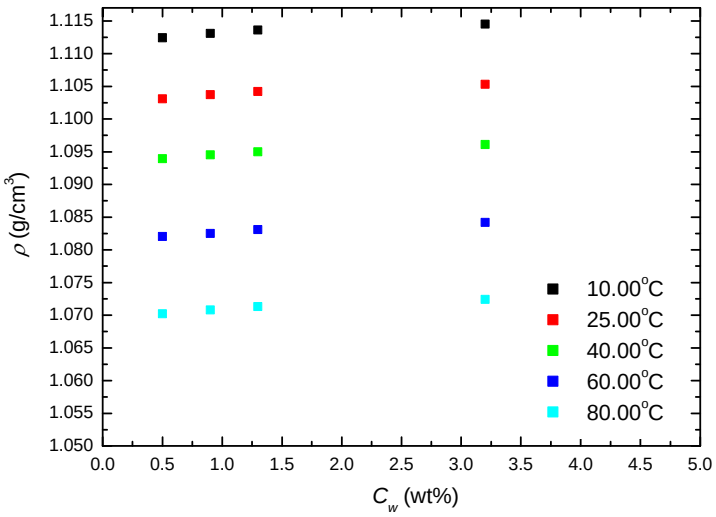

Figure 3-3b. Water content C_w dependence of the density for pullulan/EmimAc solution at different temperatures.

3-3 Summary.

In this section the density of the pullulan/BmimCl, AmimCl and EmimAc were measured in linear relations increasing concentration of pullulan from dilute to concentrated region up to 16 wt%. By using the results of density, the concentration c in wt% could be converted to C in g/cm^3 what will play an important supplementary function database for the properties of the pullulan/ILs solutions.

3-4 Reference

1) Ferry JD, "*Viscoelastic Properties of Polymers*", 3rd ed, (1980), John Wile & Sons Inc, NY.

2) Fredlake CP, Crosthwaite JM, Hert DG, Aki SNVK, and Brennecke JF, *J. Chem. Eng. Data*, **49**, 954-964, (2004).

3) Sastry S, *Nature,* **409**, 164-167, (2001).

4) Lapasin R, Pricl S, "*Rheology of industrial polysaccharides: theory and applications"* (1995). Blackie Academic and Professional, Glasgow.

5) Li W, Zhang Z, Han B, Hu S, Xie Y, and Yang G, *J. Phys. Chem. B*, **111***,* 6452−6456, (2007).

6) Yang Q, Zhang H, Su B, Yang Y, Ren Q, and Xing H, *J. Chem. Eng. Data,* **55***,* 1750–1754, (2010).

7) Wu D, Wu B, Zhang YM, and Wang HP, *J. Chem. Eng. Data,***55***,* 621–624. (2010).

Chapter 4 Intrinsic viscosity of pullulan in ionic liquid solutions

4-1 Introduction.

In this section, intrinsic viscosity [η] of pullulan in ILs is determined from the data obtained by conventional rheometry. Nine pullulan samples with different molecular weights and narrow MWD are dissolved into BmimCl and EmimAc. For the sample P-400, [η] of pullulan in AmimCl is also determined. Oscillatory and steady shear flow measurments are carried out for dilute solutions. By using zero shear viscosities of solutions and solvent, intrinsic viscosity of pullulan in BmimCl and EmimAc are determined by the ordinary method. The Mark-Houwink-Sakurada equations are determined from the data and compared with that in aqueous solution.[1) ~4)]

4-2 Results and discussion.

4-2-1 Viscoelastic measurements.

It is known that ILs strongly adsorb moisture resulting in decrease of solvent viscosity.[5) ~ 7)] The effect of moisture adsorption was examined for both ILs by repeating viscosity measurements for a certain time interval combined with Karl-Fisher titration before and after the measurement. In the most significant case, about 10 % decrease of viscosity was observed for BmimCl after 2 hours duration time even treated in the N_2 box mentioned in Experiment part. The initial water content 1.8 wt% was increased to 2.2 wt% in this case. However, the decrease of viscosity for BmimCl became

less than 5 % when the measurement time is kept within 30 min. The effect of moisture adsorption behavior of AmimCl was almost the same as that for BmimCl. For EmimAc, the effect was much less than for BmimCl. The effect of moisture adsorption become almost negligible when the measurement time is kept within 30 min.

Since ILs are glass forming liquids and BmimCl showed apparent shear thinning at high shear rate[8), 9)], effect of viscoelastic properties of ILs for polymer solutions are also examined. Figure 4-1 shows double logarithmic plots of storage (G') and loss (G'') moduli against ω for BmimCl. The observed G' values are close to the lower detection limit of the rheometer, while oscillatory measurements itself was difficult for EmimAc because of the low viscosity. Thus, we can conclude that G' of ILs are negligibly small compared to those of dilute polymer solutions shown below. Together with the steady flow data shown later, we can conclude that ILs can be treated as ordinary solvents for the viscoelastic measurements even for dilute solutions.

Figure 4-2a and b shows examples of double logarithmic plots of G' and G'' vs ω for pullulan/BmimCl and pullulan/EmimAc solutions, respectively. The data are shifted along the vertical axis by 10^n to avoid overlapping. In the lower ω region, typical terminal region behaviors ($G' \propto \omega^2$ and $G'' \propto \omega$) for uniform viscoelastic liquid is observed. In the higher ω region, the ω dependencies of G' and G'' changed from $\omega^{2/3}$ to $\omega^{1/2}$ with the increase of concentrations. It can be

considered that the viscoelastic properties of pullulan in ILs change from Zimm-like to Rouse-like behaviors.[10) ~ 12)] The details of dynamic viscoelastic properties will be reported in section 5.

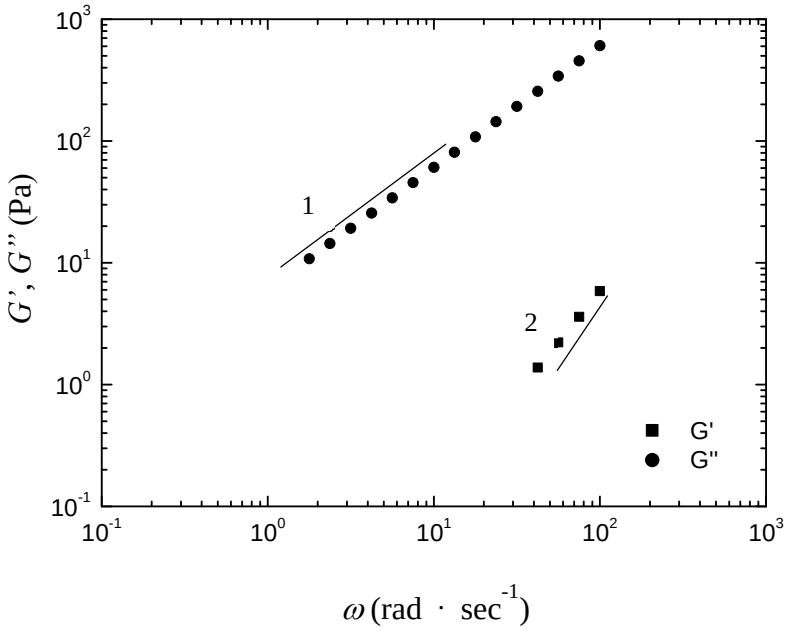

Figure 4-1. Double logarithmic plots of G' and G'' vs ω for BmimCl (water content 0.6%) at 25 °C.

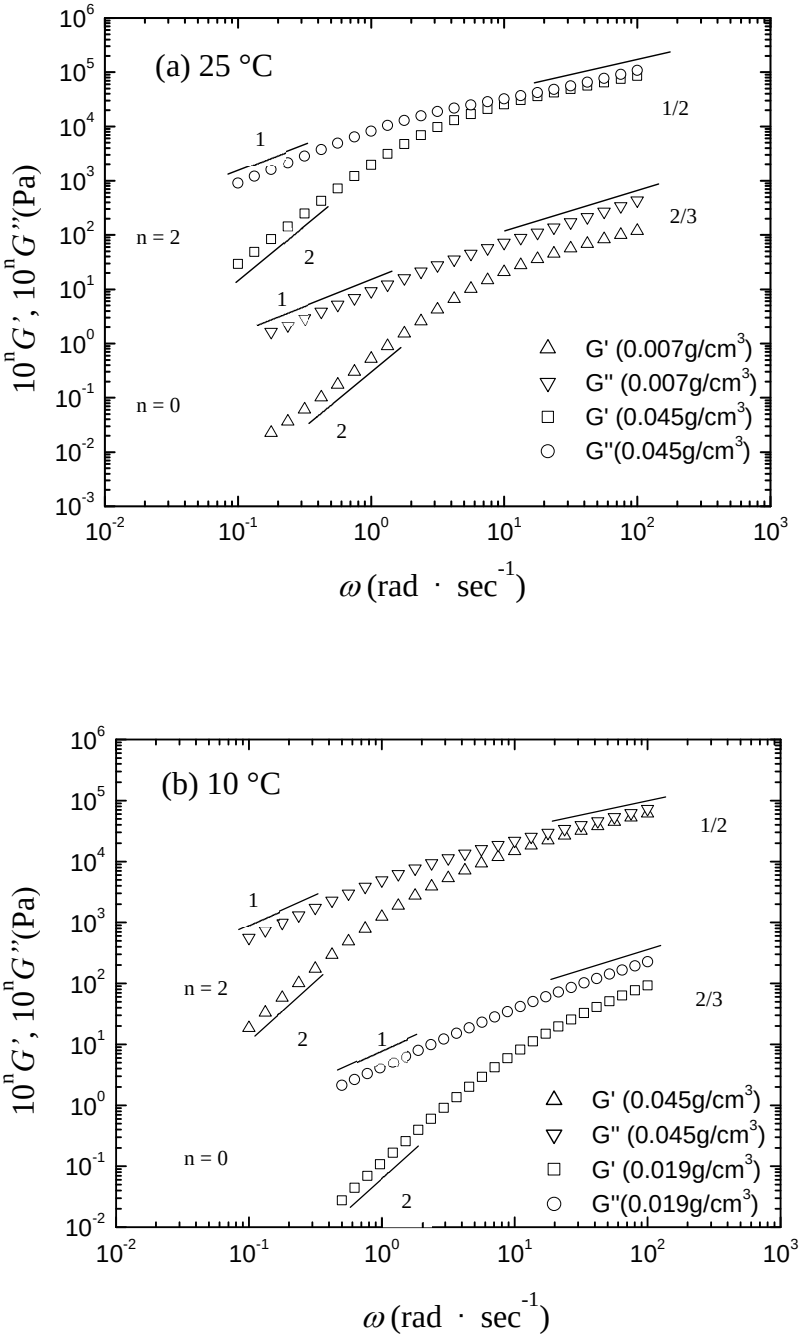

Figure 4-2. Double logarithmic plots of *G'* and *G''* vs ω for (a) pullulan (P-400)/BmimCl and (b) pullulan (P-800)/EmimAc solutions with different concentrations at 25 °C and 10 °C, respectively. Symbols are denoted in the figure.

Figure 4-3a and b show examples of shear rate ($\dot{\gamma}$) dependences of steady shear viscosity $\eta(\dot{\gamma})$ for (a) pullulan (P-400, P-100)/BmimCl solutions with different concentrations at 25 °C and (b) at different temperatures for C = 0.019 g/cm^3 (P-400, 1.8 wt%). Figure 4-4 shows examples of $\dot{\gamma}$ dependence of $\eta(\dot{\gamma})$ for pullulan (P-400, P-100)/EmimAc solutions. The Newtonian behaviors are clearly observed in lower shear rate region as denoted by horizontal lines, while shear thinning is observed in higher shear rate region for all of the BmimCl solutions. With the increase of the concentration or the decrease of the temperature, the Newtonian viscosities increase and the shear thinning regions shift to slightly lower shear rates. For the lower molecular weight sample (P-100) at lower concentrations, shear thinning become less evident. For the pullulan (P-100)/EmimAc solutions, no shear thinning behavior is observed even in higher concentrations than in BmimCl, which can be attributed to the lower viscosity of EmimAc compared to that of BmimCl. In these figures, typical $\eta(\dot{\gamma})$ data for solvent ILs are shown for comparison. It is clear that solvents do not show shear thinning and solvent viscosity η_s can be obtained with good accuracy. Above mentioned shear thinning behavior can be regarded as the behavior of ordinary polymer solutions. All these features are typical ones observed for the ordinary dilute polymer solutions.

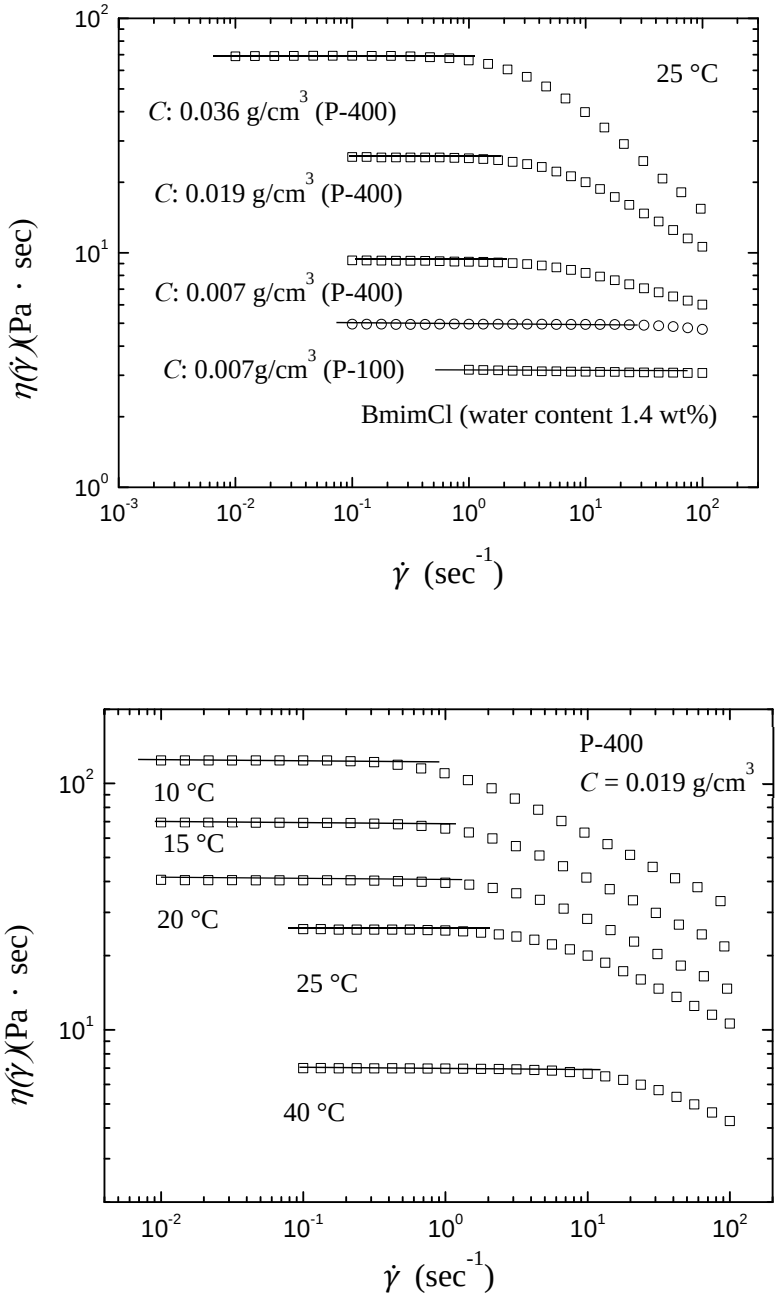

Figure 4-3. Double logarithmic plots of $\eta(\dot{\gamma})$ vs $\dot{\gamma}$ for pullulan/BmimCl solutions. Samples, concentrations, and temperatures are denoted in the figure.

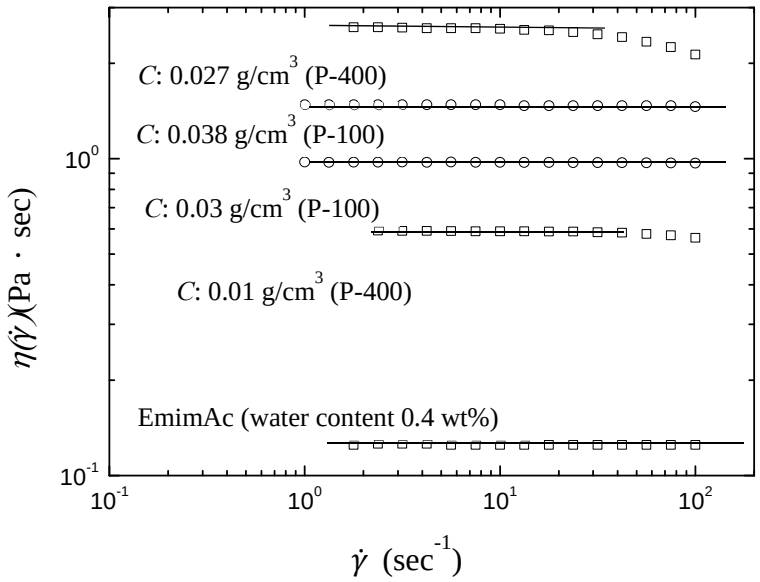

Figure 4-4. Double logarithmic plots of $\eta(\dot{\gamma})$ vs $\dot{\gamma}$ for pullulan/EmimAc solution with different concentrations at 25 °C. Samples and concentrations are denoted in the figure.

Figure 4-5 shows comparison between complex viscosity $\eta^*(\omega)$ and $\eta(\dot{\gamma})$ for pullulan/BmimCl solutions in the Newtonian region. It is clear that both data well coincide with each other and the Newtonian region in the steady shear measurements can cover wide range of $\dot{\gamma}$. For pullulan/EmimAc solution, qualitatively the same behavior was observed. From these data, zero shear viscosity η^0 of solutions are obtained. At still lower *C*, where the oscillatory data are not obtained with good accuracy, η^0 are obtained by steady shear measurements alone.

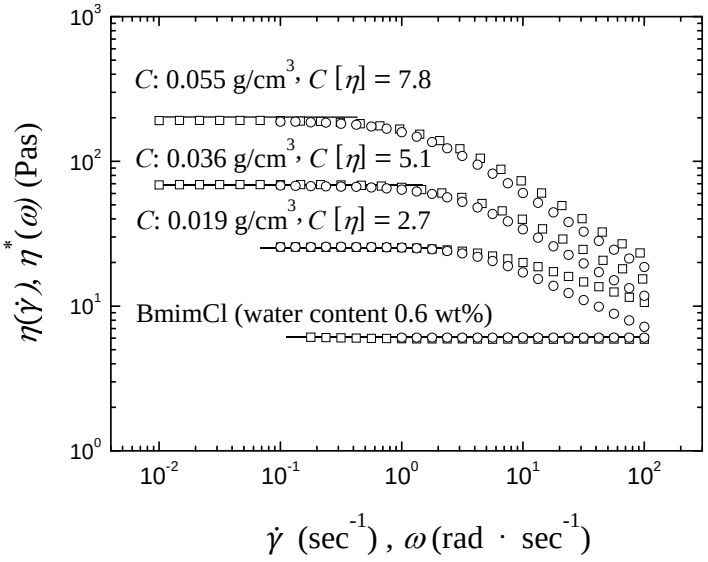

Figure 4-5. Comparison between $\eta(\dot{\gamma})$ and $\eta^*(\omega)$ for pullulan (P-400)/BmimCl solutions with different concentrations at 25 °C. The square symbols denote $\eta(\dot{\gamma})$ and the circle symbols denote $\eta^*(\omega)$. Concentrations are denoted in the figure.

4-2-2 Intrinsic Viscosity and Mark-Houwink-Sakurada equations of pullulan in ILs

From η_s and η^0, relative viscosity η_{rel} ($=\eta^0/\eta_s$) and specific viscosity η_{sp} ($=\eta_{rel}$-1) are calculated to obtain intrinsic viscosity of polymers in IL solutions.[13), 14)] Plots of η_{sp}/C and $\ln\eta_{rel}/C$ vs C, is used to determined $[\eta]$ by extrapolation to zero concentration shown by two straight lines in Figure 4-6. For all of the solutions, $[\eta]$ at 25 °C were determined while $[\eta]$ at 10 °C and 40 °C are obtained for tested samples as shown in Figure 4-7 to 4-12. The obtained $[\eta]$ are tabulated in Table 4-1. The values of $[\eta]$ for P-400 in BmimCl and AmimCl are almost same around 150 cm^3/g, and $[\eta]$ in BmimCl and

AmimCl do not show apparent change with the temperature, implying that solvent power of all three ILs for pullulan are constant in the tested range of temperature though only one sample is measured in AmimCl.

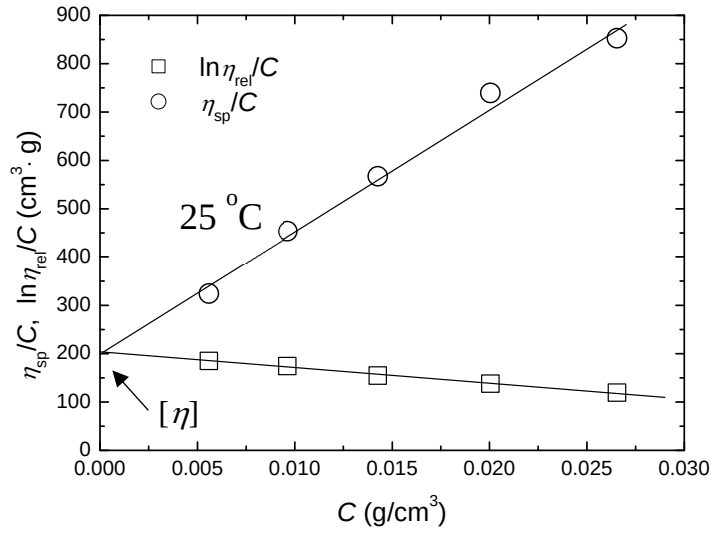

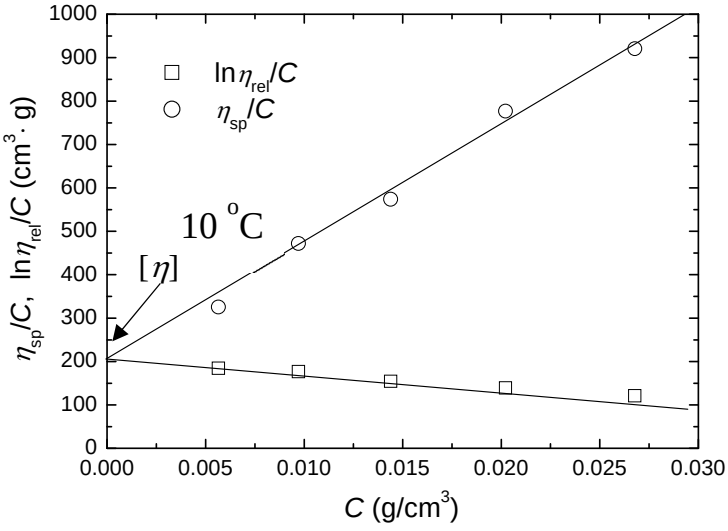

Figure 4-6. Concentration dependence of η_{sp}/C and $\ln\eta_{rel}/C$ for pullulan (P-400) in EmimAc solution. The temperatures are denoted in the figure.

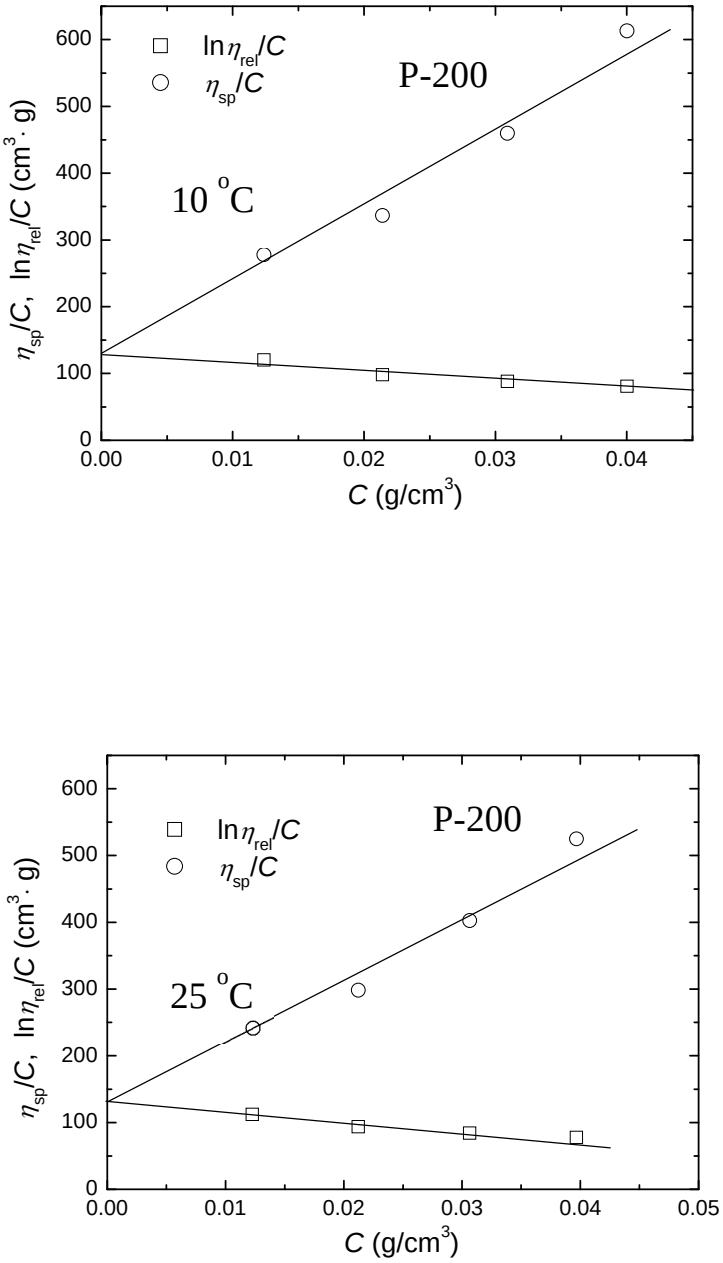

Figure 4-7. Concentration dependence of η_{sp}/C and $\ln\eta_{rel}/C$ for pullulan (P-200) in EmimAc solution. The temperatures are denoted in the figure.

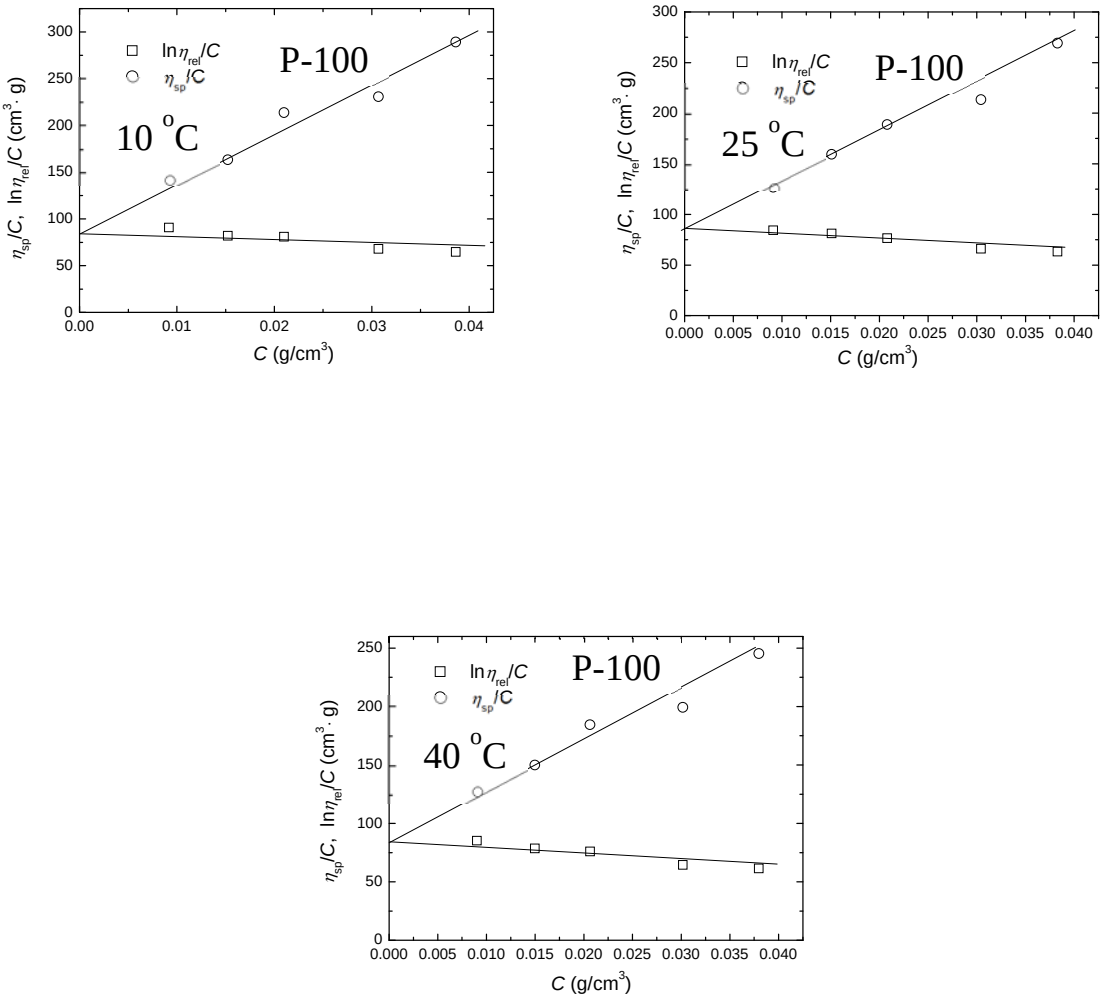

Figure 4-8. Concentration dependence of η_{sp}/C and $\ln\eta_{rel}/C$ for pullulan (P-100) in EmimAc solution. The temperatures are denoted in the figure.

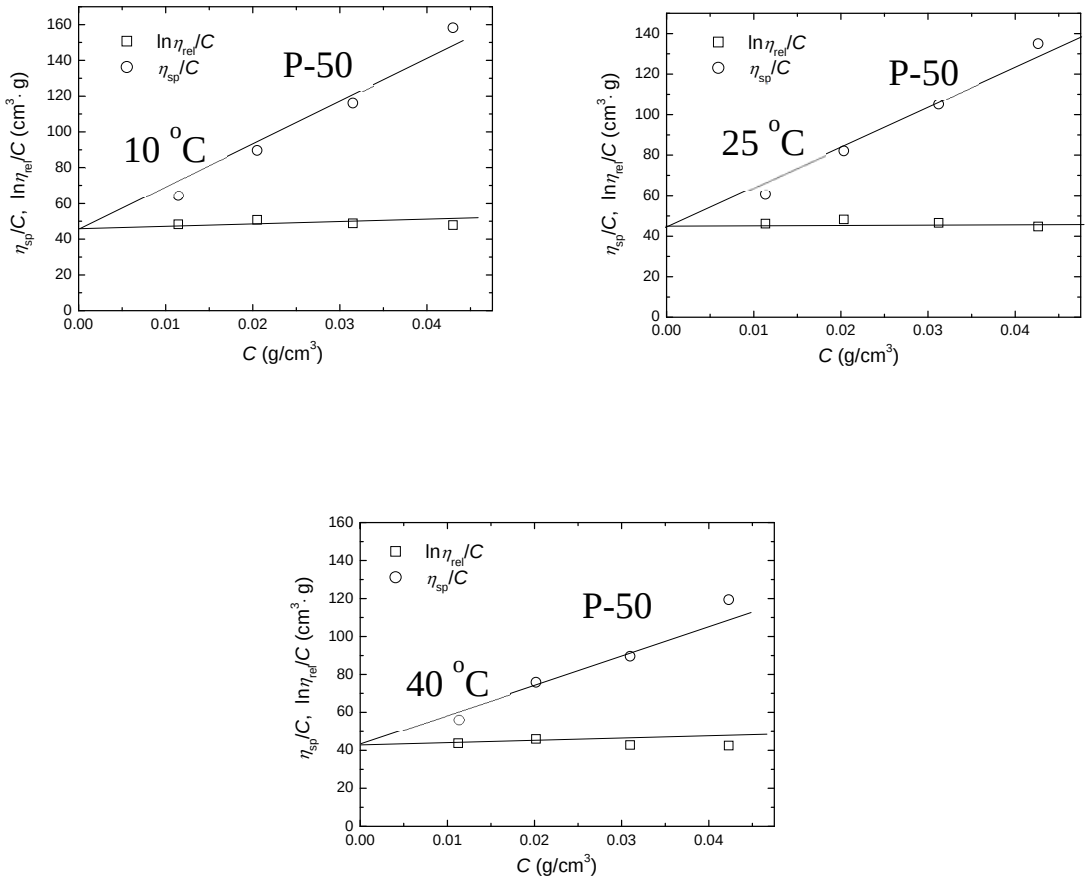

Figure 4-9. Concentration dependence of η_{sp}/C and $\ln\eta_{rel}/C$ for pullulan (P-50) in EmimAc solution. The temperatures are denoted in the figure.

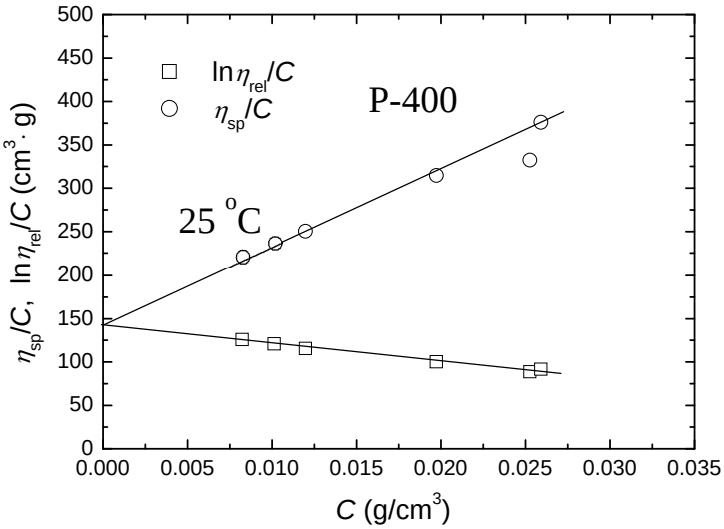

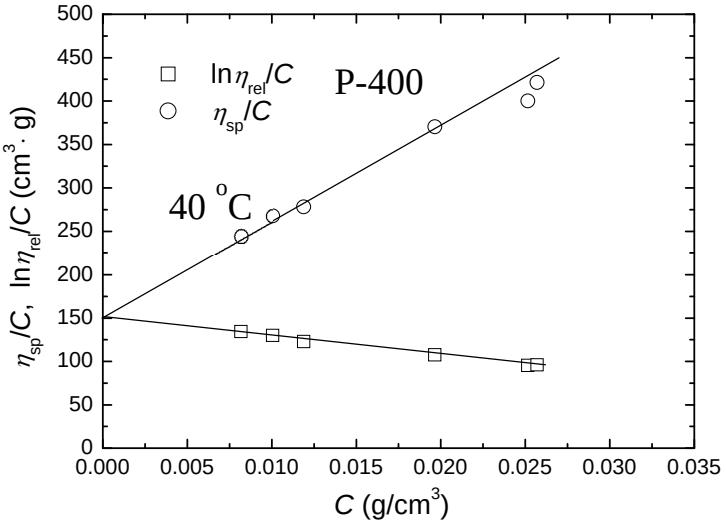

Figure 4-10. Concentration dependence of η_{sp}/C and $\ln\eta_{rel}/C$ for pullulan (P-400)

in BmimCl solution. The temperatures are denoted in the figure.

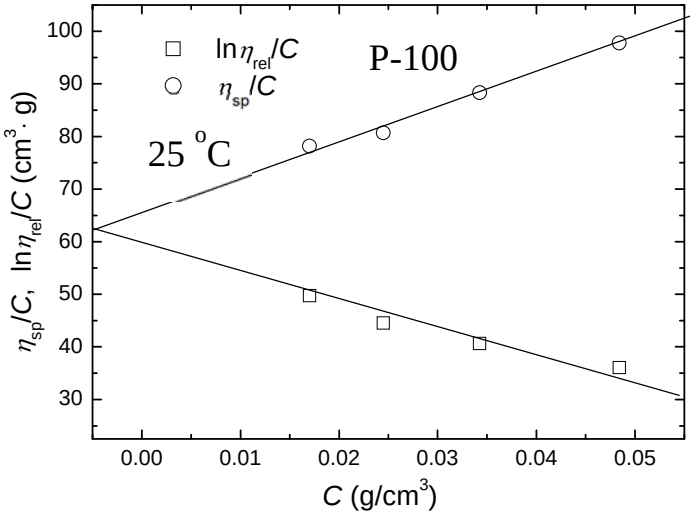

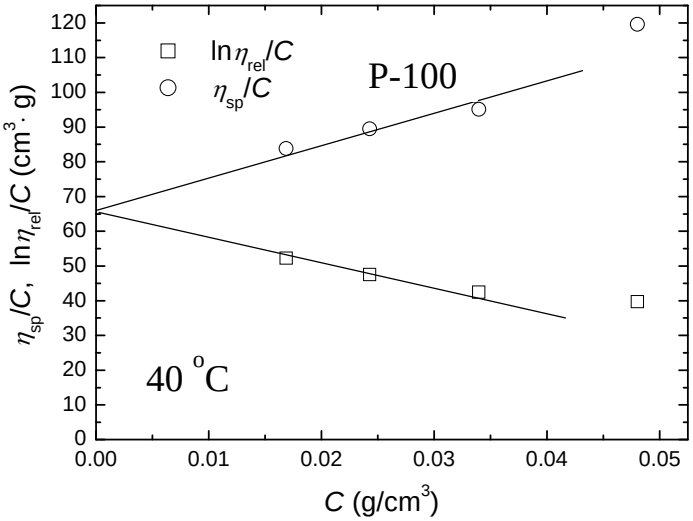

Figure 4-11. Concentration dependence of η_{sp}/C and $\ln\eta_{rel}/C$ for pullulan (P-100) in BmimCl solution. The temperatures are denoted in the figure.

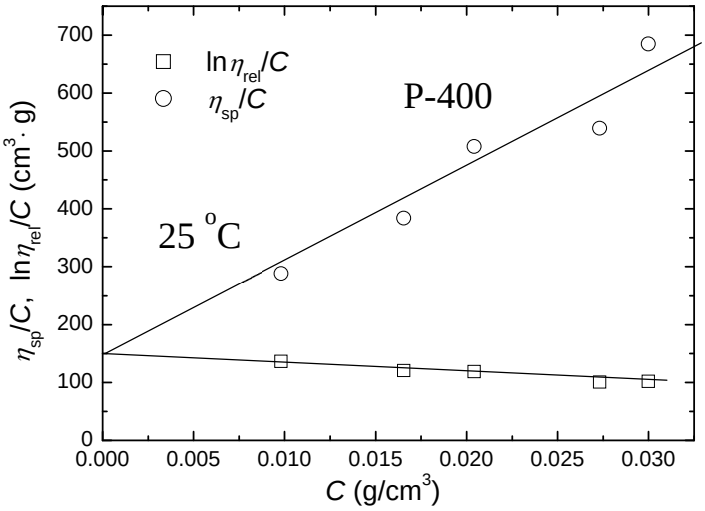

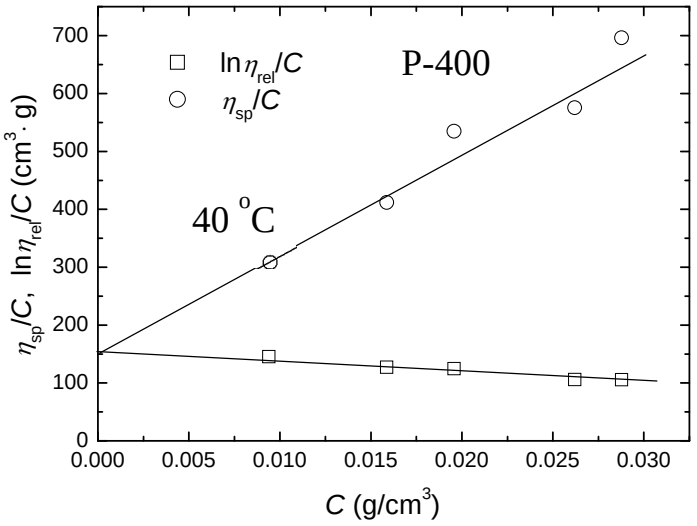

Figure 4-12. Concentration dependence of η_{sp}/C and $\ln\eta_{rel}/C$ for pullulan (P-400)

in AmimCl solution. The temperatures are denoted in the figure.

Table 4-1 Molecular characteristics of pullulan samples and their intrinsic viscosities in ILs

Molecular characteristics of pullulan samples			Intrinsic viscosities of pullulan in ILs				
Sample codes	M_w (α)	M_w/M_n (β)	[η](25°C) BmimCl	[η](40°C) BmimCl	[η](10°C) EmimAc	[η](25°C) EmimAc	[η](40°C) EmimAc
P-1300	1.33×10^6	1.37	----	----	440	450	----
P-800	7.88×10^5	1.23	268	----	265	280	----
P-400	3.93×10^5	1.10	147	150	206	203	----
P-200	2.12×10^5	1.13	119	----	128	130	----
P-100	1.13×10^5	1.13	63	65	84	85	83
P-50	4.88×10^4	1.07	45	----	46	46	44
P-20	2.28×10^4	1.07	22	----	----	25	----
P-10	1.18×10^4	1.10	17	----	----	18	----
P-5	0.59×10^4	1.09	12	----	----	----	----

(α): M_w determined by ultra-centrifugal sedimentation equilibrium, reported by manufacture.

(β): M_w/M_n determined by size exclusion chromatography, reported by manufacture.

Figure 4-13 shows double logarithmic plots of $[\eta]$ against M_w in two IL solutions at 25 °C. The data for aqueous solutions[1)] and the Mark-Houwink-Sakurada (MHS) equations determined at above M_w = 48kg/mol (slope: 0.67) and below $M_w \cong$ 30kg/mol (slope: 0.5) are also shown for comparison. It is evident that $[\eta]_{EmimAc} > [\eta]_{BmimCl} > [\eta]_{water}$, where subscripts denote the solvent, in high M_w region, say higher than 20 – 30kg/mol. In low M_w region, $[\eta]_{EmimAc}$ and $[\eta]_{BmimCl}$ almost coincide with but very slightly higher than $[\eta]_{water}$ compared at the same M_w. The data at M_w < 30kg/mol can be represented by $M_w^{0.5}$ dependence. It can be concluded that pullulan molecules behave as typical flexible polymer in ILs.[14), 15)] The excluded volume effects in ILs are somewhat stronger than in aqueous solution and become negligible at somewhat lower M_w than in aqueous solution.

By using the data at M_w > 20kg/mol, the MHS equation in BmimCl and EmimAc is obtained as eqs (18) and (19), respectively, by the least square method.

$$[\eta] = (0.038 \pm 0.02)M^{0.65\pm0.05} \quad (\text{in cm}^3\ \text{g}^{-1}) \tag{18}$$

$$[\eta] = (0.034 \pm 0.01)M^{0.67\pm0.02} \quad (\text{in cm}^3\ \text{g}^{-1}) \tag{19}$$

Since the data in Figure 4-13 for IL solutions are scarce and slightly scattered compared to the data in aqueous solutions, the uncertainty of the above equations become somewhat larger than those

for aqueous solutions. But we can still conclude that measurement of [η] by rheometer is a promising method for characterization of so-called insoluble polymers in ILs.

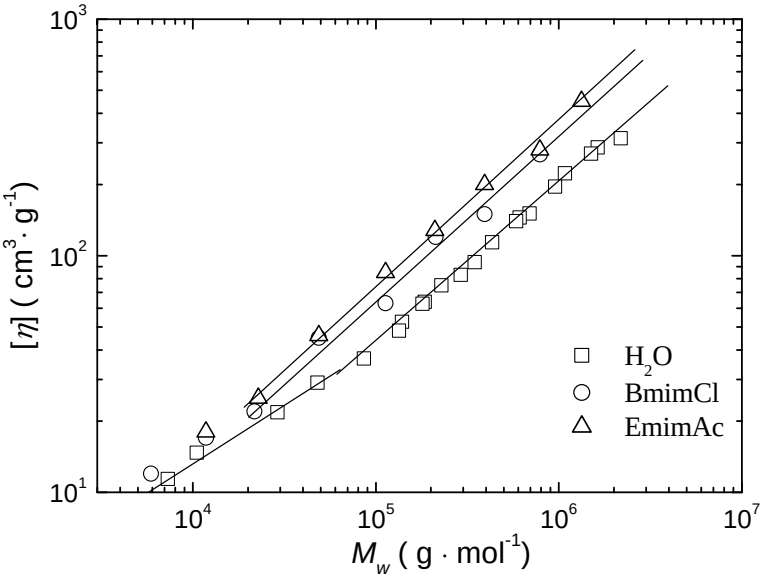

Figure 4-13. The molecular weight dependence of [η] for pullulan in BmimCl, EmimAc, and aqueous solutions at 25 °C

4-3 Summary.

By using the Oscillatory and steady shear flow measurments, zero shear viscosities are determined consistently. Shear thinning behavior was observed under steady shear flow while the viscoelastic behavior changed from Zimm like to Rouse like with the increasing concentration. These features are typical ones observed for the ordinary dilute polymer solutions.

From zero shear viscosities of solutions and solvent, intrinsic viscosity of pullulan in ILs are determined by the ordinary method. It was observed that ILs were good solvent for pullulan. And the Mark-Houwink-Sakurada equations are also determined. Therefore it is a promising method to determine [η] by rheometer for characterization of so-called insoluble polymers in ILs.

4-3 Reference

1) Kato T, Okamoto T, Tokuya T, Takahashi A, *Biopolymers*, **21**, 1623-1633, (1982).

2) Kato T, Katsuki T, Takahashi A, *Macromolecules*, **17**, 1726-1730, (1984).

3) Kawahara K, Ohta K, Miyamoto H, Nakamura S, *Carbohydr. Polym*, **4**, 335-356, (1984).

4) Nishinari K, Kohyama K, Williams PA, Phillips GO, Burchard W, and Ogino K, *Macromolecules*, **24**, 5590-5593, (1991).

5) Rodrı´guez H, and Brennecke JF, *J. Chem. Eng. Data,* **51***,* 2145−2155, (2006).

6)Li W, Zhang Z, Han B, Hu S, Xie Y, and Yang G, *J. Phys. Chem. B*, **111***,* 6452−6456, (2007).

7) Wu D, Wu B, Zhang YM, and Wang HP, *J. Chem. Eng. Data,***55***,* 621–624, (2010).

8) Maeda A, Inoue T, Sato T, *Macromolecules*, **46**, 7118, (2013).

9) Takada A, Imaichi K, Kagawa T, and Takahashi Y, *J. Phys. Chem. B*, **112**, 9660-9662, (2008).

10) Rouse PE, *J Chem Phys,* **21**, 1272, (1953).

11) Zimm BH, *J Chem Phys,* **24**, 269, (1956).

12) Ferry JD, "*Viscoelastic Properties of Polymers*", 3rd ed, (1980), John Wile & Sons Inc, NY.

13) Huggins ML, *J. Am. Chem. Soc*, **64**, 2716–2718, (1942).

14) Lapasin R, Pricl S, "*Rheology of industrial polysaccharides: theory and applications"* (1995). Blackie Academic and Professional, Glasgow.

15) Doi M, Edwards SF, "*The Theory of Polymer Dynamics"* (1986). Oxford University Press, Oxford.

Chapter 5 Viscoelastic properties of dilute pullulan/ILs solutions

5-1 Introduction.

In this section, the dynamic viscoelastic properties of pullulan ILs solutions with different molecular weights and concentrations in the non-entangled regions are examined in comparison with the Rouse-Zimm theory[1)-3)] with correction terms[4)], which almost perfectly expressed the data for standard polystyrenes in good solvents. Based on the results in previous sections, measurements are carried out at only one or two temperatures for each solution keeping short measurement time to avoid possible moisture adsorption. The selected measuring temperatures are high enough from glass transition temperature of solvent and solution so that we can minimize the possible effect of the glass relaxation.[5)] Concentration dependences of fitting parameters in the correction term, zero-shear viscosity η^0 and steady state compliance J_e obtained from the data are discussed. Estimation of the molecular weight of sample by fitting the dynamic moduli data to the theory is also tested.

5-2 Results and discussion.

5-2-1 Comparison with the Rouse-Zimm theory.

As mentioned in section 1-2, it should be emphasized that the original Rouse-Zimm (RZ) theory argues the viscoelastic behavior of isolated Gaussian chain in solution.[3] Though the all ILs used in this study are good solvents for pullulan, excluded volume effects become negligible for low M samples (M_w < 30kg/mol) as clarified from intrinsic viscosity data in section 4. Therefore, applicability of RZ theory is first tested for low M sample, P-20 (22.8kg/mol) in BmimCl.

Figure 5-1 shows double logarithmic plots of G' and $G''-\eta_s$ vs ω for P-20 in BmimCl. G' and the G" can be expressed as the following general formulae[3), 4)],

$$G''(\omega) = \frac{CRT}{M}\sum_{P=1}^{N}\frac{\omega\ \tau_P}{1+\omega^2{\tau_P}^2} + G''(solvent) \qquad (5)$$

$$G'(\omega) = \frac{CRT}{M}\sum_{p=1}^{N}\frac{\omega^2{\tau_P}^2}{1+\omega^2{\tau_P}^2} \qquad (6)$$

$$G''(solvent\ ) = \omega\eta_s \qquad (7)$$

$$\tau_p = \frac{\tau_{RZ}}{p^{\alpha}} \qquad (8)$$

where α = 2 corresponds to non-draining limit[1], while α = 1.5 corresponds to free-draining limit.[2] The relaxation time τ_{RZ} can be obtained phenomenologically from the inverse value of ω at the crossing point of G' and $G''-\eta_s$, as shown in Figure 5-1. By using the experimental values of this system, fitting of the RZ theory to the data can be tested in principle by using α and N as fitting

parameters. Figure 5-2 shows comparison between the data and calculated values according to the RZ theory, with arbitral choice of N when N is higher than 50, there was the Rouse calculation is more close to the data but the difference between two extreme calculations is not so large and fitting cannot be tested well without the data in higher ω regions, which is not accessible in this case. Therefore, we test the fitting further with other data as mentioned below.

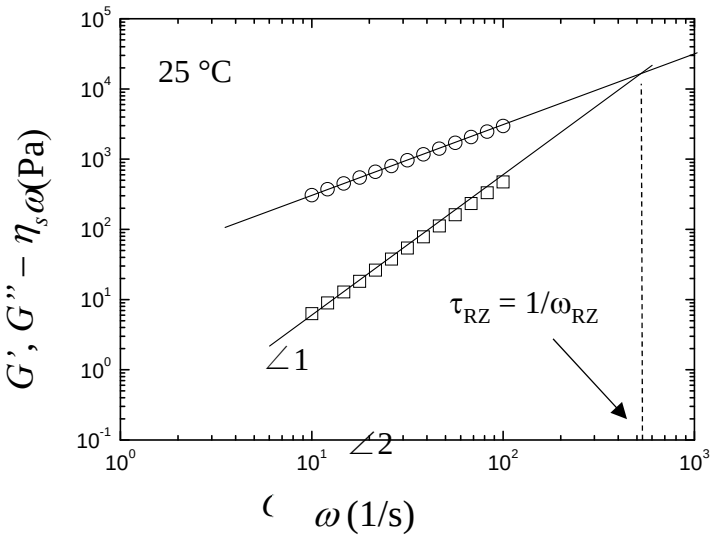

Figure 5-1. Double logarithmic plots of G' and G''-$\eta_s\omega$ against ω for pullulan (P-20)/BmimCl. The squares denote G' while the circles denote G'' -$\eta_s\omega$. Experimental conditions are denoted in the figure. The relaxation time τ_{RZ} of this system can be determined from the crossing point of dynamic data.

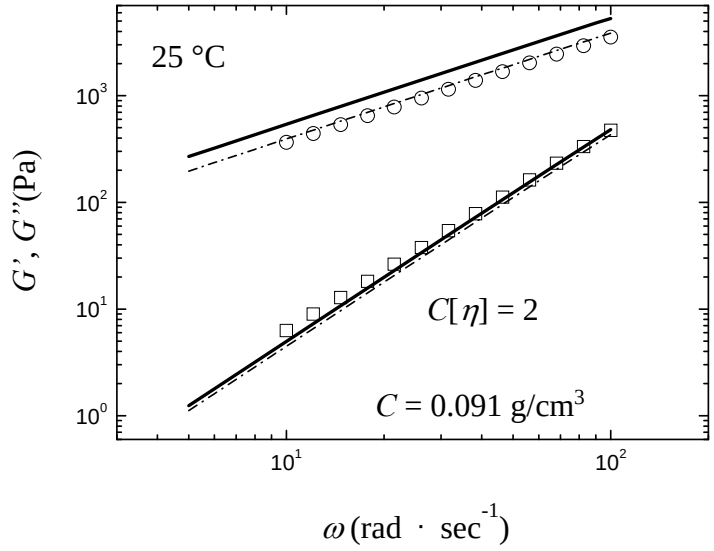

Figure 5-2. Comparison between dynamic viscoelastic data of pullulan (P-20)/BmimCl in Figure 1 and the calculation from Rouse-Zimm model at 25 °C. The square symbols denote *G*', the circle symbols denote *G*''. Solid lines denote the calculation with $\alpha = 1.5$ and the dashed lines denote those with $\alpha = 2$.

Figure 5-3 shows examples for double logarithmic plots of *G'* and *G''* for higher *M* sample, P-200 in BmimCl with different α. Note that $C[\eta]$ =1.6 for (a) and $C[\eta]$ =1.8 for (b), denoting that polymer chains in these solutions are not overlapped. It seems that α range from1.8 to 2 provide better fitting to the data in (a), though the most apparent deviation between the data and RZ theory observed

in the figure are almost the same. A similar result is also obtained for the data in (b). Note that the good fitting results with N = 50 in eqs. 5 and 6 are obtained and there was almost no practical difference when N exceeds 50. Therefore, 50 is chosen as the value of N for all data in this chapter.

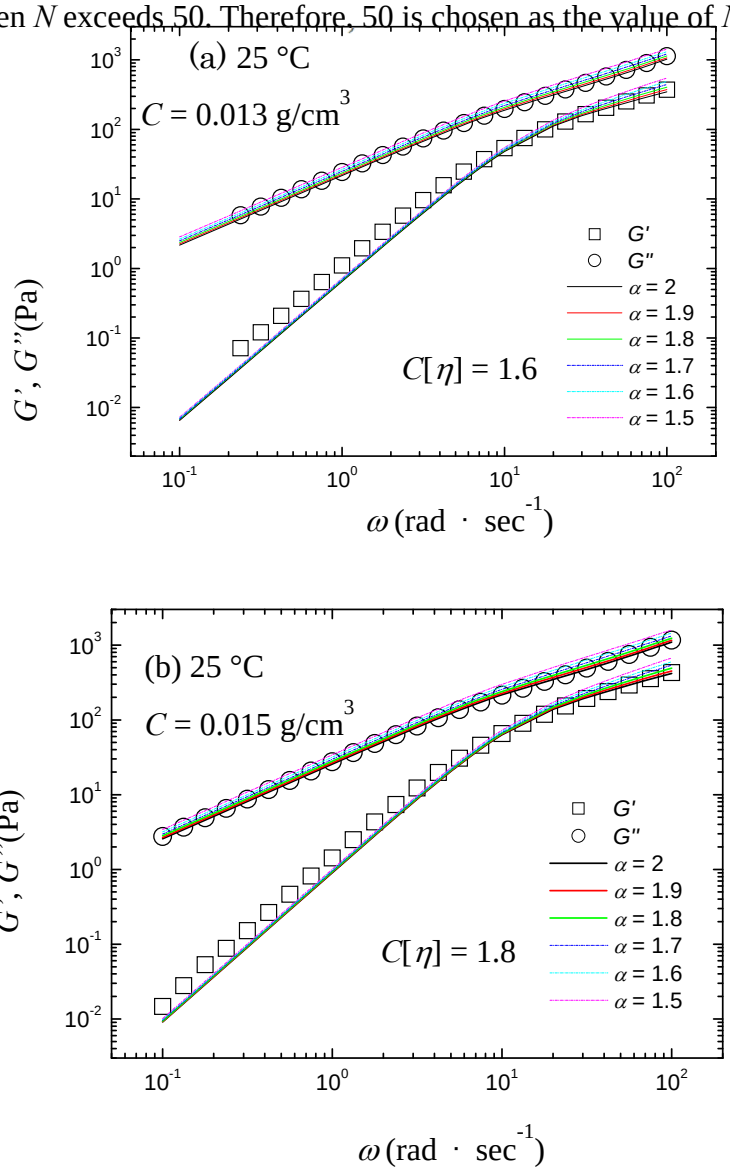

Figure 5-3. Comparison between dynamic viscoelastic data of pullulan (P-200)/BmimCl solutions with different C, and the calculation from Rouse-Zimm model at 25 °C with different α.

Concentrations are denoted in the figure.

Similar behavior is also observed for (P-400)/BmimCl and AmimCl solutions as shown in Figure 5-4, when $C[\eta]$ is greater than 2.

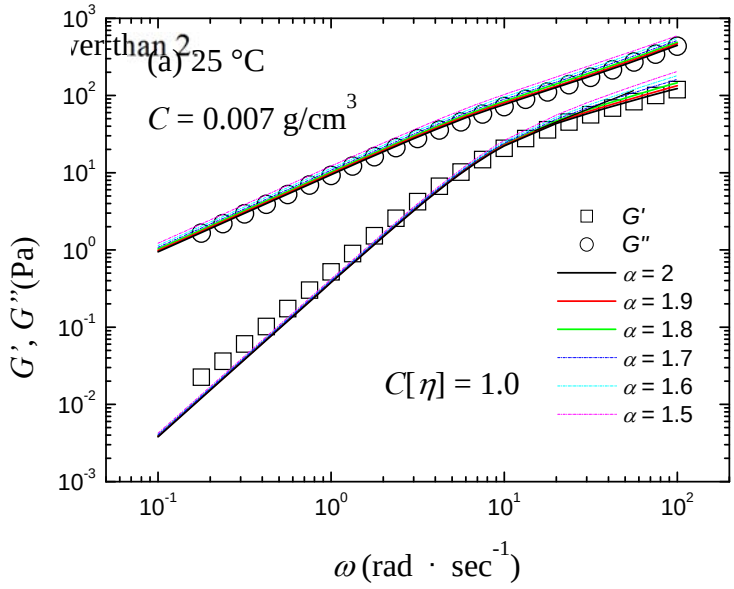

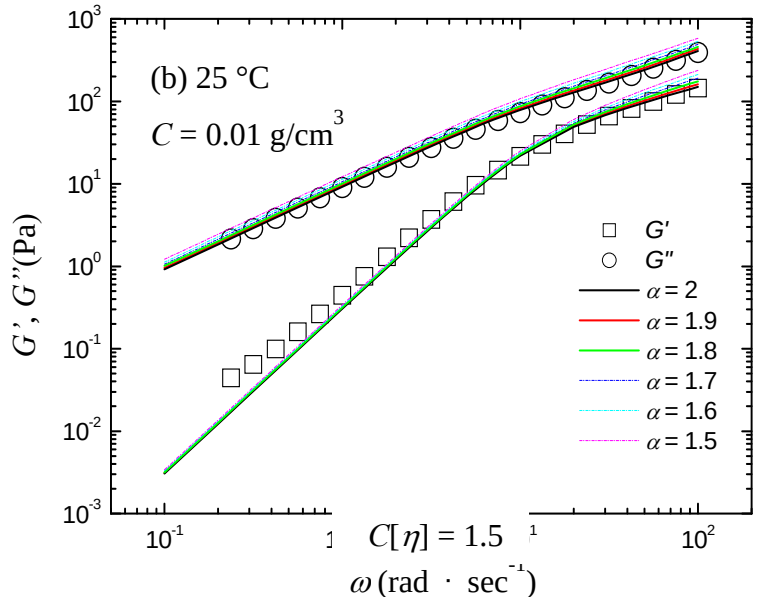

Figure 5-4. Comparison between dynamic viscoelastic data of pullulan (P-400)/BmimCl (a) and AmimCl (b), and the calculation from Rouse-Zimm model at 25 °C with different α. Concentrations

are denoted in the figure.

Figure 5-5 shows an example of G^* for higher $C[\eta]$ solution. It was clarified that $\alpha = 2$ can be fixed for solutions when $C[\eta]$ is higher than 2. It should be also noted that τ_{RZ} become practically the same with the value obtained by the following equation in those cases,

$$\tau_p = \frac{6\eta_0 M}{\pi^2 p^2 C\mathrm{R}T} \qquad (9)$$

Here, $p = 1$ corresponds to the longest relaxation time.

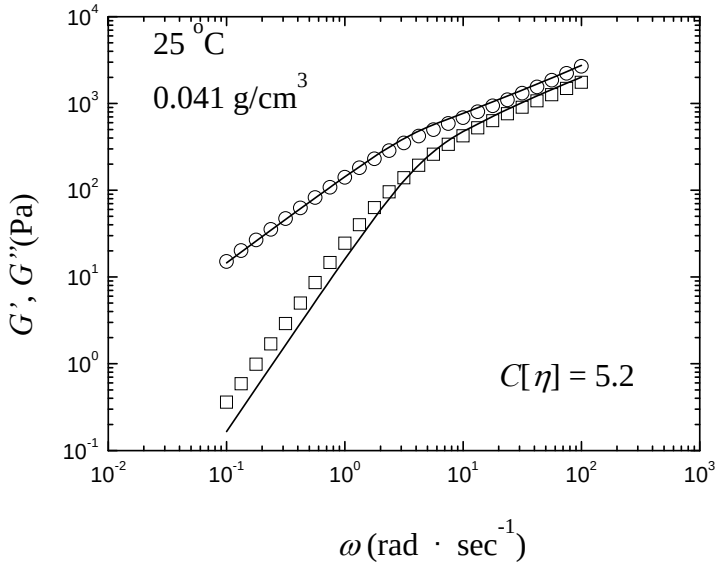

Figure 5-5. Comparison between dynamic viscoelastic data of pullulan (P-200)/BmimCl solutions and the calculation from Rouse-Zimm model at 25 °C. Concentration is denoted in the figure. The square symbols denote *G'*, the circle symbols denote *G''*. The solid line denote calculation for original

Rouse-Zimm model.

According to the above results, it can be considered that the viscoelastic behavior of pullulan/ILs solutions in dilute region can be well approximated by Rouse-Zimm theory using the only adjustable parameter α near the overlapping concentration threshold.[6) - 8)] However, when degree of the polymer coil overlapping $C[\eta]$ is increased, small deviations between experimental and calculated values of G^* at higher ω region observed as shown in Figure 5-5 become slightly larger. The reason for this deviation may include a few different effects such as the local motions of units, solvating environment and so on. The further analysis of such effects is far beyond the purpose of this thesis. The important point is that the fitting of data with RZ theory become the best at around $C[\eta]$ = 1-2, just below the overlapping threshold. As mentioned before, τ_{RZ} can be determined from the crossing point of dynamic data (Figure 5-1) and the equation 9. For the concentration below the overlapping threshold, the value from equation 9 are slightly higher than that from the data (Figure 5-1). However for the concentrations higher than overlapping concentration ($C[\eta]$ >2), both relaxation times well coincide with each other as shown in Table 5-1. Note that the value of τ_{RZ} calculated from equation 9 is not suitable for the concentration below the overlapping threshold.

Table 5-1 τ_{RZ} from data and calculation in BmimCL solutions,

$C[\eta]$	τ_{RZ} (data)	τ_{RZ} (calculate)
	P-400	
1.04	0.090	0.128
2.85	0.125	0.129
3.75	0.126	0.126
5.325	0.190	0.188
6.75	0.210	0.195
8.25	0.337	0.34
	P-200	
1.55	0.063	0.097
1.75	0.070	0.097
2.944	0.107	0.106
3.43	0.110	0.110
4.1	0.143	0.148
5.248	0.180	0.179
6.784	0.24	0.234

Even in those cases, correction term is needed for more good representation of *G*' data at low ω region as described below. Osaki *et al*.[4] systematically studied *G** data for standard polystyrene in a good solvent and employed correction term called long-time (LT) term to get a good fit at low ω;

$$G'_{LT} = G_{LT} \frac{\tau_{LT}^{\ 2}\omega^2}{1+\tau_{LT}^{\ 2}\omega^2} \qquad (10)$$

$$G''_{LT} = G_{LT} \frac{\tau_{LT}\omega}{1+\tau_{LT}{}^{2}\omega^{2}} \qquad (11)$$

$$G_{LT} = QC[\eta]\frac{C\mathrm{R}T}{M} \qquad (12)$$

$$\tau_{LT} = P\tau_{RZ} \qquad (13)$$

where Q and P being adjustable parameters (Q = 0.09 and P = 5 in their study). The calculated G" with and without LT term are practically the same, while G' data in the lower frequency region can be well fitted by addition of the LT term.

The calculated values with LT term are also compared with experimental data of pullulan in three ILs, as represented in Figure 5-6 to Figure 5-8. In the calculation, the best fit was obtained with P nearly equal 5 and Q values shown as slopes for the straight lines in plots of $G_{\mathrm{LT}}M/C\mathrm{R}T$ vs $C[\eta]$, shown in Figure 5-9.

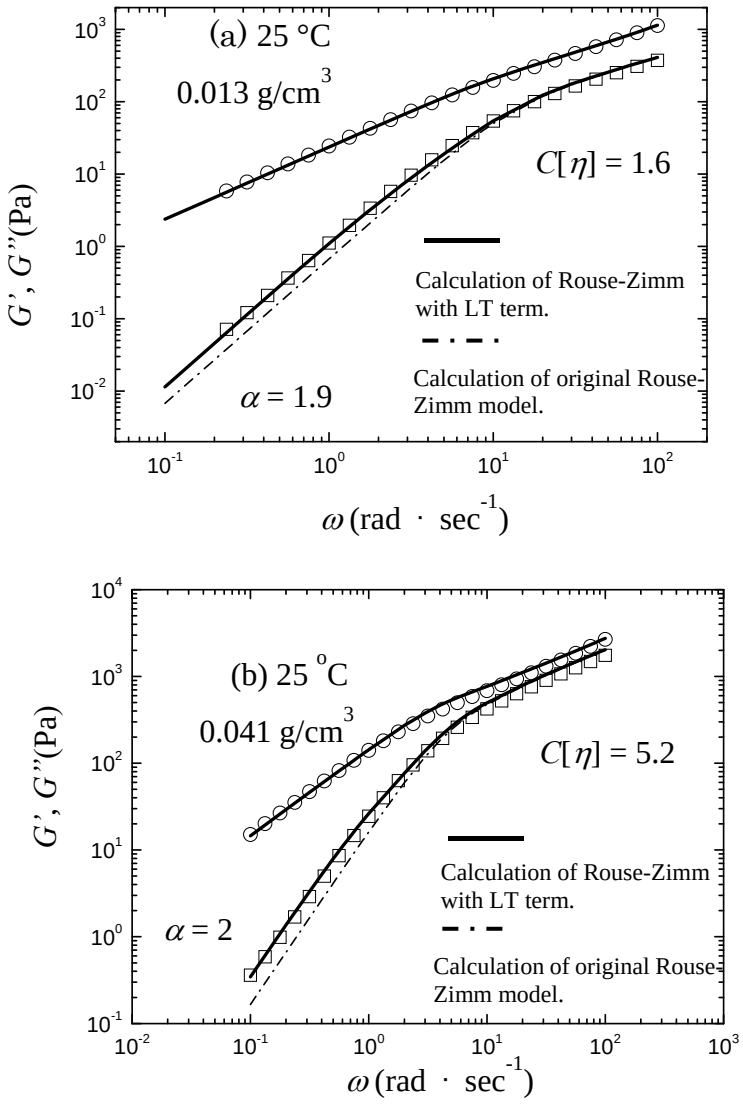

Figure 5-6. Comparison between dynamic viscoelastic data of pullulan (P-200)/BmimCl solutions with different concentrations and the calculation from Rouse-Zimm model at 25 °C. Concentrations are denoted in the figure. The square symbols denote *G*', while the circle symbols denote *G*''. The broken lines denote the calculation of original Rouse-Zimm model, and the solid lines denote those

for Rouse-Zimm model with LT term. Note that broken and solid lines for *G*" are completely superimposed.

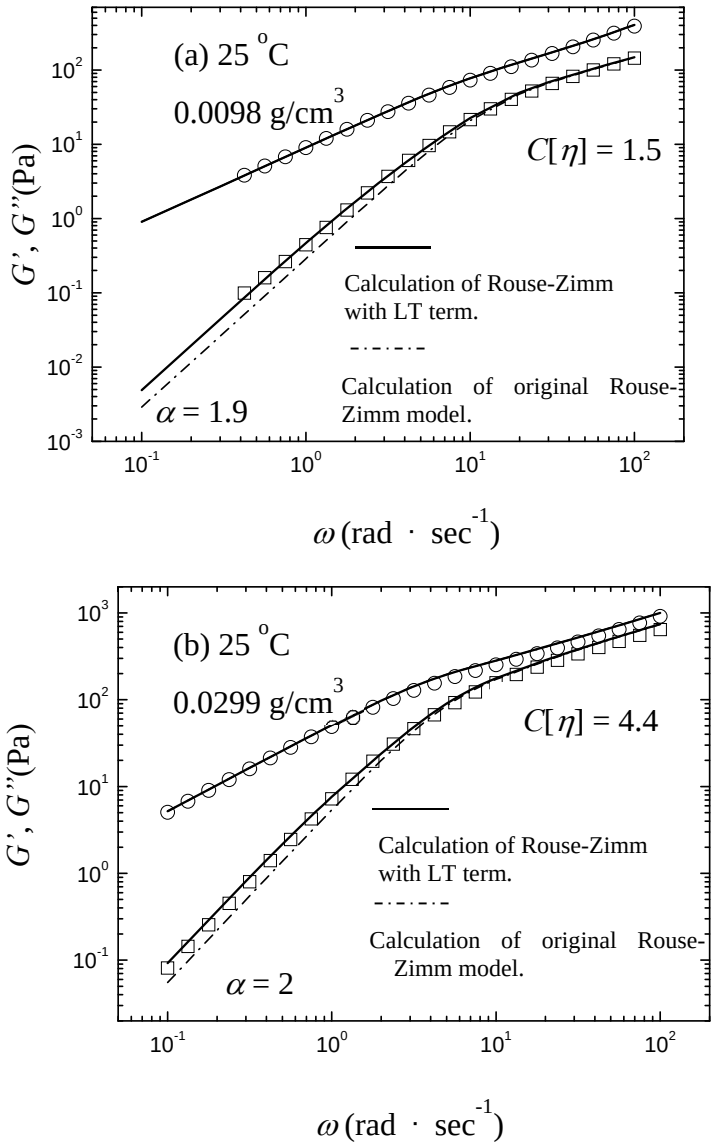

Figure 5-7. Comparison between dynamic viscoelastic data of pullulan (P-400)/AmimCl solutions with different concentrations and the calculation from Rouse-Zimm model at 25 °C. Concentrations are denoted in the figure. The square symbols denote *G*', while the circle symbols denote *G*''. The broken lines denote the calculation of original Rouse-Zimm model, and the solid lines denote those

for Rouse-Zimm model with LT term. Note that broken and solid lines for *G*" are completely superimposed.

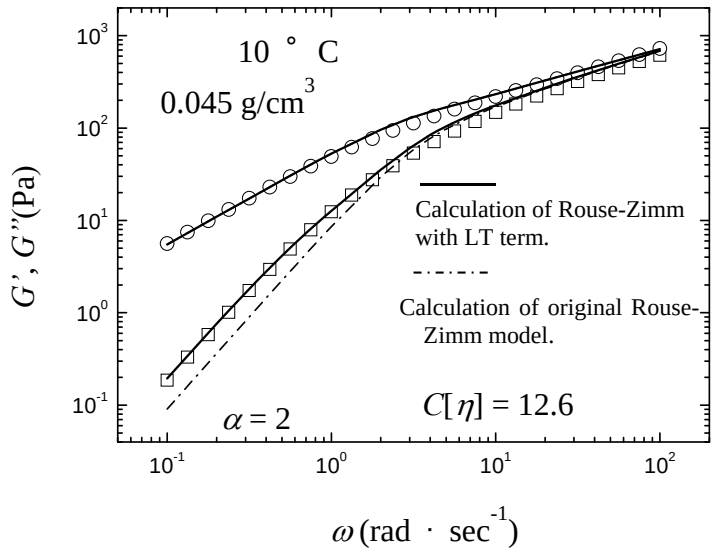

Figure 5-8. Comparison between dynamic viscoelastic data of pullulan (P-800)/EmimAc solution and the calculation from Rouse-Zimm model at 10 °C. Concentrations are denoted in the figure. The square symbols denote *G'*, while the circle symbols denote *G"*. The broken lines denote the calculation of original Rouse-Zimm model, and the solid lines denote those for Rouse-Zimm model with LT term. Note that broken and solid lines for *G*" are completely superimposed.

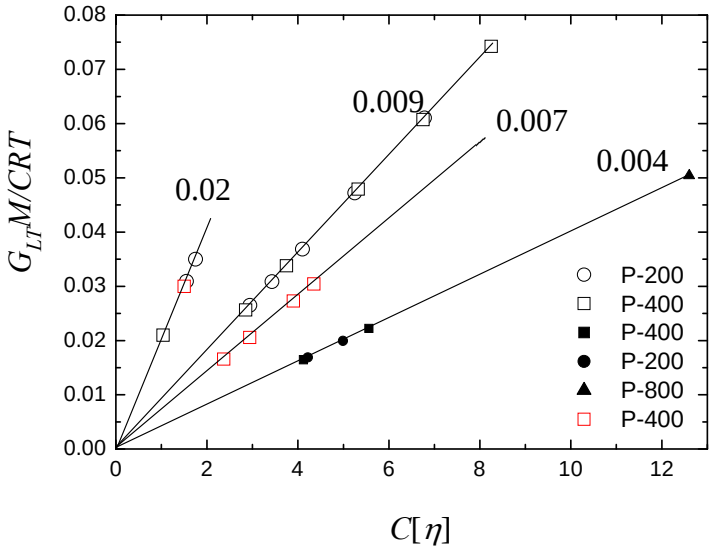

Figure 5-9. Plots of $G_{LT}M/CRT$ vs $C[\eta]$. Slopes of straight lines denoted in the figure corresponds to Q values. Symbols are denoted in the figure. The unfilled black symbols denote the data in BmimCl, the unfilled red symbols denote the data in AmimCl and the filled symbols denote those in EmimAc.

By using the modified equations with LT term, the fitting of *G'* in lower frequency region become almost perfect as shown above. It is clear in Figure 5-9 that *Q* changes suddenly at around $C[\eta] = 2$. Inoue et al.[9), 10)] reported that polymer chains overlap with each other at $C[\eta] = 2.5$ and the hydrodynamic interactions are shielded by the overlapping of polymer chains for polystyrene in a good solvent. For pullulan/BmimCl solutions, *Q* is 0.02 at $C[\eta] < 2$ and *Q* changes to be 0.009 at $C[\eta] > 2$, qualitatively consistent with the results reported by Inoue et al.[9), 10)]

It was explained that when the concentration *C* is lower than the overlapping concentration, the hydrodynamic interaction affects among isolated polymer chains. With increase of *C*, the polymer chains become slightly overlapped with each other so that the hydrodynamic interactions between chains are shielded.[6)-8)] In the semidilute region, hydrodynamic correlation length, which preserves the nature of polymer solvent interactions, becomes the unit length and rather weak interactions among them exist. Therefore the parameter *Q* changed to much lower value in the semidilute region. This idea is consistent with the understanding for thermodynamic properties of polymer solutions, in which radius of gyration and static correlation (or alternatively, screening) length are used as unit length for dilute and semidilute regions respectively. Note that critical overlapping concentration is

also consistent for hydrodynamic and static behaviors of polymer solution.

For the solutions with $C[\eta] > 2$, the parameter α is always 2 and Q is 0.007 for AmimCl and 0.004 for EmimAc which is slightly lower than that in pullulan/BmimCl solution, 0.009. It seems that the dynamic interaction effects in these ILs act somewhat different ways, which may be related to expansion forms of viscoelastic parameters (η^0 and J_e) in dilute solutions. The further discussions of above parameters in relation with the expansion forms are far beyond from analysis in this thesis. In the next sub-section, the concentration dependence of η^0 and J_e are discussed in comparison with those of synthetic polymer solutions.

5-2-2 Concentration dependence of zero shear viscosity.

In the dilute and semidilute regions, the zero shear viscosity η^0 can be discussed by the reduced form, η_R^0 defined as $\eta_R^0 = \eta_{sp}/C[\eta]$, where $\eta_{sp} = (\eta^0-\eta_s)/\eta_s$, by the expansion form (equation 4 in section 1) of $C[\eta]$ as

$$\eta_R^0 = 1 + k'C[\eta] + \cdots$$

Here k' is Huggins constant. It is widely accepted that k' is close to 0.35 in good solvents and close to 0.8 in θ solvents for synthetic linear polymers.[11) - 13)] Since all ILs used in this study can be regarded as good solvents for pullulan, it is expected that all viscosity data can be expressed by the expansion form assuming $k' = 0.35$.

Figure 5-10 shows double logarithmic plots of η_R^0 vs $C[\eta]$ for all viscosity data obtained in this study together with the calculated line with k' = 0.35. It is clear that all data are approximately expressed by the calculated line, though they are somewhat scattered compared to the similar plots for synthetic model polymers in good solvents. This is due to the larger experimental errors in this study for viscosity measurements at low concentrations; viscosities of synthetic polymers can be measured by capillary methods with small errors (usually ±0.3%), which cannot be used for IL solutions. It can be pointed out that the data seems to deviate from the calculated line at around $C[\eta]$ = 10, also consistent with the data for synthetic polymers denoting the entanglement effects at higher $C[\eta]$. From these results, it can be concluded that the viscosity behavior of pullulan/IL solutions in dilute region can be quite similarly expressed as those for synthetic linear model polymers.[13)]

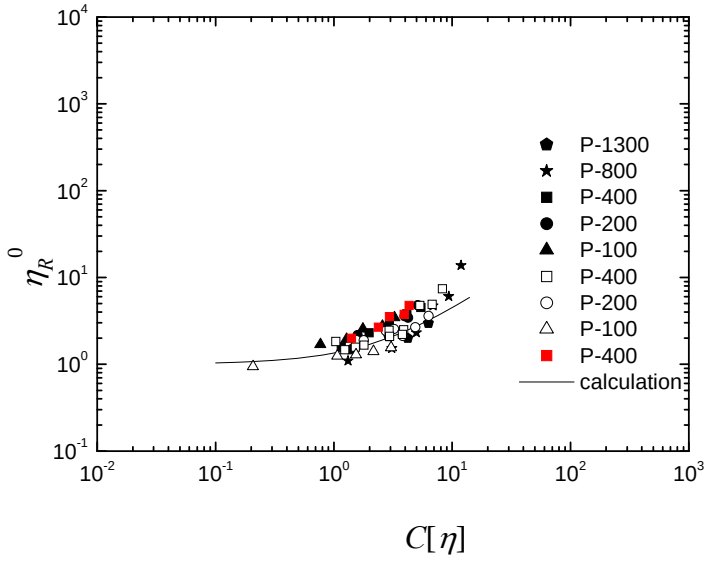

Figure 5-10. Double logarithmic plots of η_R^0 vs. $C[\eta]$ for pullulan in ILs. The unfilled symbols denote

data for BmimCl, the filled red symbols denote data for AmimCl and the filled black symbols denote data for pullulan/EmimAc solutions. The solid line denote the calculation with k' = 3.5.

5-2-3 Concentration dependences of the steady-state compliance.

The steady-state compliance J_e, which is a measure of elastic recoil of polymer chain, can be obtained as low-frequency limiting value of $(G'/\omega^2)/(G''/\omega)^2$.[14] The theoretical value for Zimm model is 0.206 and that for Rouse model is 0.4 at infinite dilution. To discuss the data at finite concentration, reduced steady-state compliance J_{eR} defined by following equation is employed.

$$J_{eR} = \frac{J_e C \mathrm{R} T}{M}\left(\frac{\eta^0}{\eta^0 - \eta_s}\right)^2 \qquad (20)$$

It has been reported that J_{eR} gradually increase with increase of $C[\eta]$ for the synthetic linear polymer solutions from about 0.2 to 0.4.[3), 12), 15)]

In Figure 5-11, steady-state compliance J_e is double logarithmically plotted against $C[\eta]$ for the pullulan/BmimCl solutions. It can be seen that J_e are almost constant at low C but turn to decrease with the increasing concentration; J_e is proportional to C^{-1} for the higher M_w samples. For polystyrene solutions[15)], it is reported that J_e increases from the value for Zimm model to that for Rouse model.

Figure 5-12 shows double logarithmic plots of J_{eR} vs $C[\eta]$ for pullulan IL solutions obtained in this study. It seems that the data have a trend to slightly increase with increase of $C[\eta]$ up to $C[\eta]$ =

3 and become constant at a slightly higher value than 0.4, which is quite similar with the data for synthetic linear polymers though the increase of J_{eR} from Zimm value was not apparent because of the limitation of experimental condition. The slightly higher value than 0.4 can be regarded as effect of LT term. As a whole, it can be concluded that the viscoelastic behaviors of pullulan/IL solutions in dilute region is practically the same as those for synthetic linear model polymers.[15), 16)] This fact also supports appropriateness of application of RZ theory with LT terms.

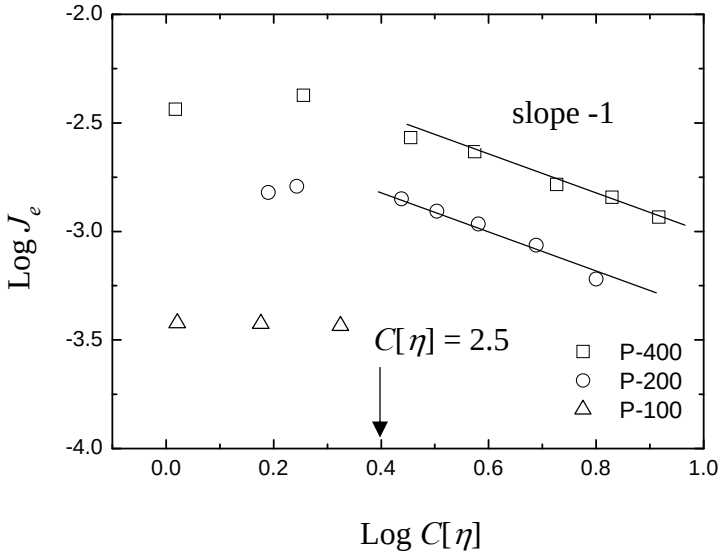

Figure 5-11. Plots of Log J_e vs Log $C[\eta]$ at 25 °C for pullulan/BmimCl solutions. Symbols are denoted in the figure. Slope of -1 denotes Rouse-like behavior.

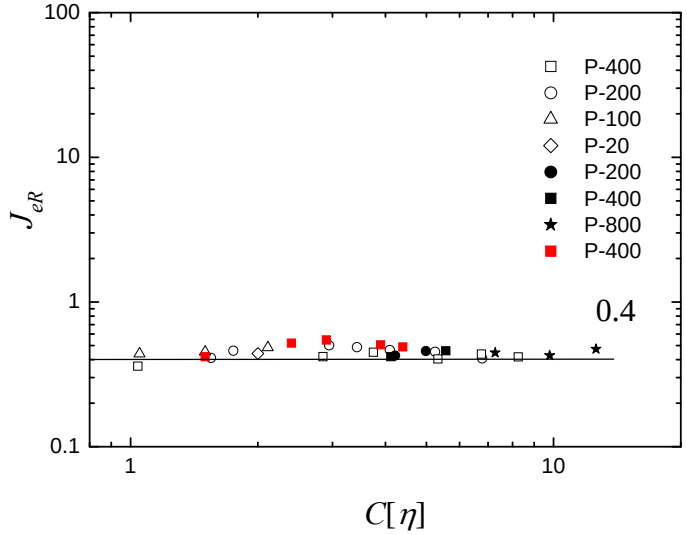

Figure 5-12. Concentration dependence of the reduced steady state compliance J_{eR} for pullulan/ILs

solutions. The unfilled symbols denote data for BmimCl, the filled red symbols denote data for pullulan/AmimCl solutions, and the filled black symbols denote data for pullulan/EmimAc solutions.

5-2-4 Estimation of the molecular weight of sample by fitting the data to Rouse-Zimm model.

According to the above results, the viscoelastic properties of pullulan in ILs are practically the same as those for the synthetic linear polymer such as polystyrene, which can be described by Rouse-Zimm model with the LT term. Therefore, fitting the experimental data to the Rouse-Zimm equations could be a method to determine the M_w for the natural polymers whose molecular weight is unknown. The precision of the Rouse-Zimm fitting is tested for pullulan/ILs solutions by floating M.

Figure 5-13 shows comparison of Rouse-Zimm fitting by using real M_w and those with $\pm$30% of M_w with $\alpha = 1.8$ and $\alpha = 2$. The fitting by using real M_w are well and showed practically the same results when α changed from 1.8 to 2. It can be seen that change in $\alpha = 1.8$ - 2 and changing M_w with ± 30% can be regarded as limiting case for the apparent deviations of data and calculations in the high frequency region, neglecting the deviation of G' at low ω. Therefore, for the sample solutions with $C[\eta]$ = 1-2, estimation of M_w from fitting can be performed within an accuracy of $\pm$30%. Note that even when $[\eta]$ cannot be estimated, we can roughly speculate the concentration region of tested solution from relaxation times. Figure 5-14 compares τ_{RZ} determined from the data (as in Figure 5-1) and calculated from eq. (9) at $C[\eta]$ >2, both relaxation times well coincide with each other.

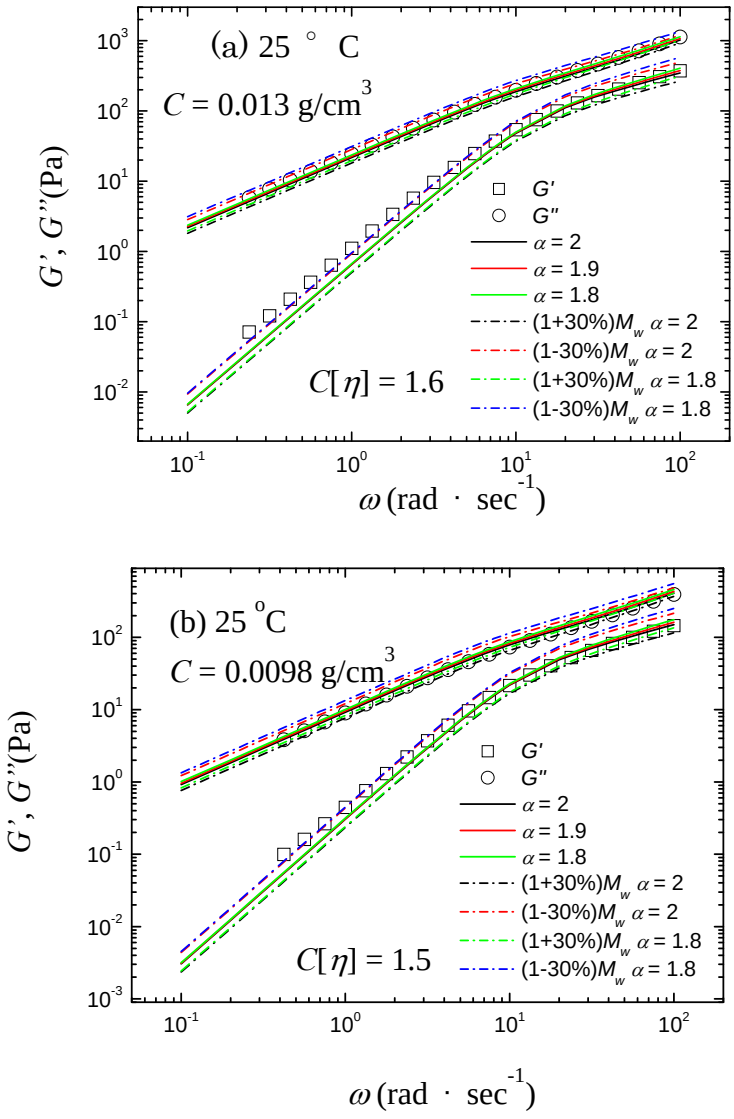

Figure 5-13. Comparison of the calculation from original Rouse-Zimm model with real M_w, and the fitting molecular weight $(1 \pm 30\%)M_w$ for pullulan (P-200)/BmimCl (a) and pullulan (P-400)/AmimCl solutions with α ranging from 1.8 to 2.

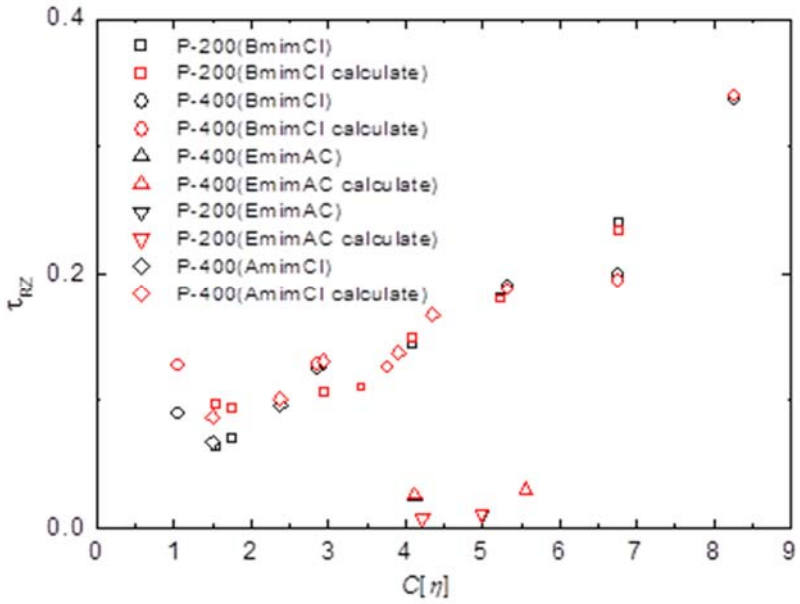

Figure 5-14. Comparison of τ_{RZ} determined from calculation eq. (9) and the experiment data (as in Figure 5-1).

For the pullulan/ILs solution at $C[\eta] > 2$, calculated values of G^* in higher frequency region become slightly higher than those of experiment with increasing C. This deviation may affect the estimation of M_w. To examine this point, M_w was slightly changed for the better match of G^* in the higher frequency region. As shown in Figure 5-15, when the M_w is set as 2.75×10^5 g/mol, which is 30% higher than the real M_w, a good match of fitting can be observed. Similar results are also observed for pullulan/AmimCl and pullulan/EmimAc solutions, as shown in Figure 5-16 and Figure 5-17 for different M_w samples. According to these results, the better fitting of the data and original RZ theory at high ω may cause 30% overestimate of M_w compared to the real one. Therefore, M_w of natural

polymer in ILs can be estimated with fixing $\alpha = 2$ and using the M_w as the only fitting parameter to the original Rouse-Zimm theory within an accuracy of $\pm 30\%$. Note that, as mentioned above, the fitting of data with RZ theory become the best at around $C[\eta]$ = 1-2, just below the overlapping threshold. With the aid of LT term may results in better estimation.

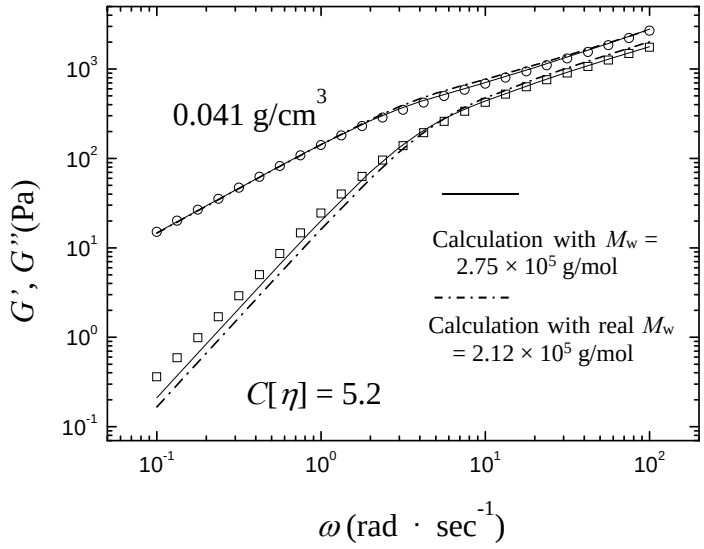

Figure 5-15. Comparison between the calculation of the original Rouse-Zimm model with real M_w = 2.12×10^5 g/mol (broken lines) and those with the best fitted value, $M_w = 2.75 \times 10^5$ g/mol (solid lines) for pullulan (P-200)/BmimCl solutions at C = 0.041g/cm^3. The square symbols denote G', the circle symbols denote G''.

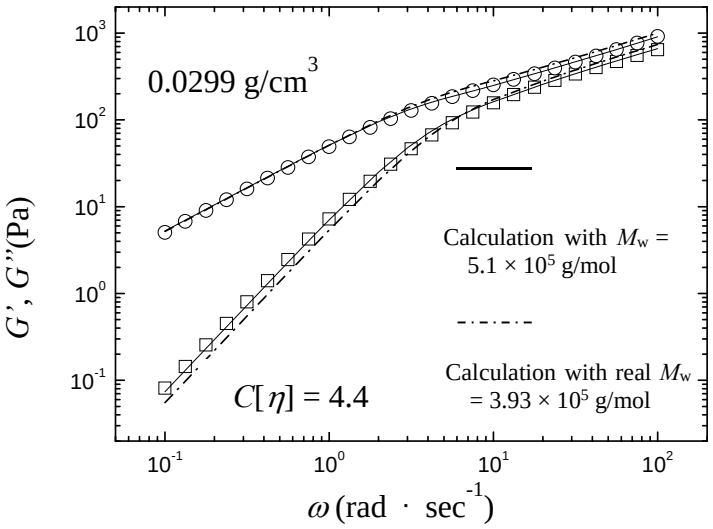

Figure 5-16. Comparison between the calculation of the original Rouse-Zimm model with real M_w = 3.93×10^5 g/mol (broken lines) and the fitted molecular weight, $M_w = 5.1 \times 10^5$ g/mol (solid lines) for pullulan (P-400)/AmimCl solutions at $C = 0.0299 g/cm^3$. The square symbols denote *G'*, the circle symbols denote *G''*.

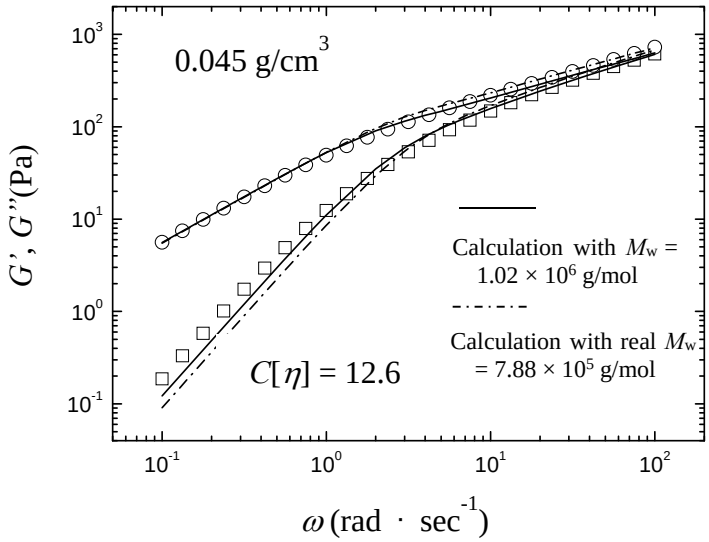

Figure 5-17. Comparison between the calculation of the original Rouse-Zimm model with real M_w = 7.88×10^5 g/mol (broken lines) and the fitted molecular weight $M_w = 1.02 \times 10^6$ g/mol (solid lines) for pullulan (P-800)/EmimAc solutions at $C = 0.045 g/cm^3$. The square symbols denote *G'*, the circle symbols denote *G''*.

5-2-5 Characterization of molecular weight for cotton by fitting the Rouse-Zimm model.

According to the above results for pulluan/ILs solutions, fitting the experimental data to the Rouse-Zimm equations can be a method to determine the M_w for the natural polymers. The idea is roughly tested by using cotton solutions. Figure 5-18 shows double logarithmic plots of *G'* and *G"* vs ω for cotton/BmimCl solution.

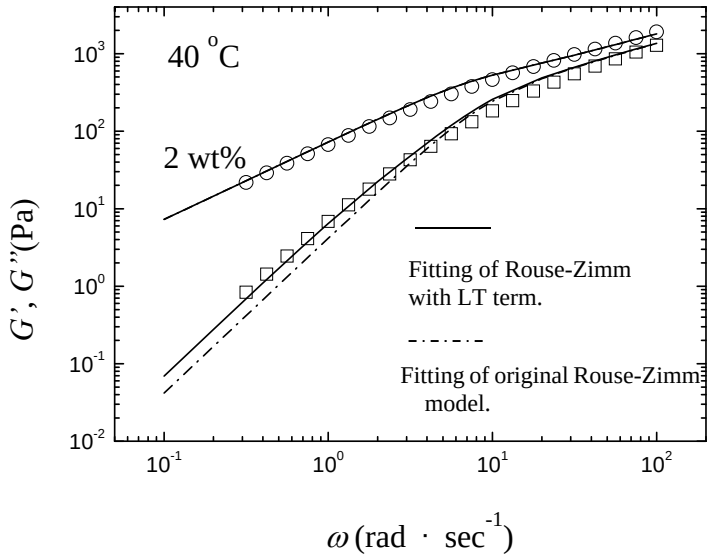

Figure 5-18. Rouse-Zimm model fitting with $M_w = 1.2 \times 10^5$ g/mol for cotton/BmimCl solution. The *c* are denoted in the figures. The square symbols denote *G*', while the circle symbols denote *G*". The broken lines denote the calculation of original Rouse-Zimm model, and the solid lines denote those for Rouse-Zimm model with LT term. Note that broken and solid lines for *G*" are completely superimposed.

As mentioned before the fitting of data with RZ theory become the best at around $C[\eta]$ = 1-2, just below the overlapping threshold. However, since $[\eta]$ of cellulose is unknown, we simply assume that the lower concentrations are suitable to use for fitting, which did not show a typical Rouse like behavior as in Figure 5-18. The relaxation times of this solution from data and calculation (eq. 9) coincided with each other meaning that $C[\eta]$ is higher than 2, though typical Rouse like behavior was not observed. By fitting the RZ theory to the experimental data, the M_w of cotton in BmimCl was determined as 1.2×10^5 g/mol. Here, $\alpha = 2$ is assumed. When the LT term is added, G' data in the lower frequency region can be well fitted. Note that wt% concentration is used for the analysis and $[\eta]$ of the cotton is assumed to be equal to that of pullulan in BmimCl, having the same M_w as estimated by fitting.

To test the fitting in the different IL, cotton was recovered from the 2wt% cotton/BmimCl solution and dissolved into AmimCl. The viscoelastic behavior of recovered cotton in AmimCl is shown in Figure 5-19. By fitting the original RZ model to the experiment data, the M_w of recovered cotton is determined as 1.1×10^5 g/mol, which is almost the same as the value obtained in BmimCl. In this fitting, $\alpha = 2$ is assumed. Furthermore, fitting with LT term resulted in good representations of the data. The values of Q are 0.02 in both of the solutions which is the same to those for pullulan/ILs solutions.

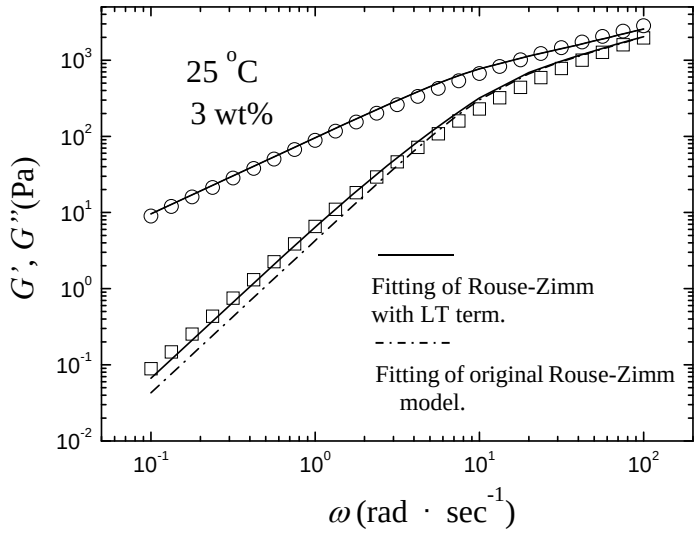

Figure 5-19. Rouse-Zimm model fitting with $M_w = 1.1 \times 10^5$ g/mol for Recovered cotton/AmimCl solution. The *c* value is denoted in the figure. The square symbols denote *G*', while the circle symbols denote *G*''. The broken lines denote the calculation of original Rouse-Zimm model, and the solid lines denote those for Rouse-Zimm model with LT term. Note that broken and solid lines for *G*" are completely superimposed.

By using the Rouse-Zimm fitting to the experiment data, the M_w of cotton could be determined conveniently. It can be a new method to obtain M_w of insoluble natural polymer, although more systematic studies are needed. That is, this method may become more precise when density of cellulose solution is measured and tested by measuring with recovered samples tested at different

concentrations and also obtaining [η]. The M_w values should be confirmed by other methods.

5-3 Summary.

The dynamic viscoelastic properties of pullulan ILs solutions in non-entangled regions coincide well with the calculation of Rouse-Zimm theory by using correction terms, which almost perfectly expressed the data for standard polystyrenes in good solvents. Concentration dependences of fitting parameters in the correction term, zero-shear viscosity η^0 and steady state compliance J_e obtained for pullulan in ILs solutions are similar to those of synthetic polymers in good solvents. All these results support that dynamic viscoelastic measurements can be used as a new characterization method to obtain M_w of insoluble natural polymers within ±30%.

References

(1) Rouse PE, *J Chem Phys,* **21**, 1272, (1953).

(2) Zimm BH, *J Chem Phys,* **24**, 269, (1956).

(3) Ferry JD, "*Viscoelastic Properties of Polymers*", 3rd ed, (1980), John Wile & Sons Inc, NY.

(4) Osaki K, Inoue T, Uematsu T, *Journa of Polymer Science: Part B: Polymer Physics,* **39**, 211–217, (2001).

(5) Maeda A, Inoue T, Sato T, *Macromolecules*, **46**, 7118, (2013).

(6) Noda I, Kato N, Kitano T, Nagasawa M, *Macromolecules*, **14**, 668, (1981).

(7) Higo Y, Ueno N, Noda I, *Polym. J.* **15**, 367, (1983).

(8) Noda I, Higo Y, Ueno N, Fujimoto T, *Macromolecules*, **17**, 1055, (1984).

(9) Inoue T, Yamashita Y, Osaki K, *Macromolecules*, **35**, 9169-9175, (2002)

(10) Osaki K, Inoue T, Uematsu T, Yamashita Y, *Journa of Polymer Science: Part B: Polymer Physics,* **40**, 1038–1045, (2002).

(11) Berry GC, Fox TG, *Adv. Polym. Sci.*, **5**, (1968).

(12) Graessley WW, *Adv. Polym. Sci*., **16**, (1974).

(13) Takahashi Y, Isono Y, Noda I, Nagasawa M, *Macromolecules*, **18***,* 1002-1008, (1985).

(14) Holmes LA, Ninomiya K, Ferry DJ, *The Journal of Physical Chemistry,* **70**, 2714-2719, (1966).

(15) Suzuki F, Hori K, Kozuka N, Komoda H, Katsuro K, Takahashi Y, Noda I, Nagasawa M, *Polymer Journal*, **18**, 12, 911-917, (1986).

(16) Takahashi Y, Noda I, Nagasawa M, *Macromolecules*, **18***,* 2220-2225, (1985).

Chapter 6. Conclusions

In this thesis, viscoelastic properties of standard pullulan samples with different molecular weights and narrow MWD in BmimCl, AmimCl, and EmimAc are studied in comparison with the behaviors of standard linear polystyrenes in dilute solutions.

In section 3, the density of the pullulan/BmimCl, AmimCl and EmimAc were measured up to 16 wt%. Linear relations of density and wt% concentration c are obtained, which can be used to convert c to C in g/cm^3. These relations are essential to examine the solution properties of the pullulan/ILs solutions.

In section 4, zero shear viscosities of pullulan/ILs solutions are obtained by using oscillatory and steady shear flow measurments. From the zero shear viscosities of solutions and solvents, intrinsic viscosity of pullulan in ILs are determined by the ordinary method. It was observed that ILs are good solvent for pullulan. Furthermore, the Mark-Houwink-Sakurada equations are also determined for BmimCl and EmimAc solutions.

In section 5, the dynamic viscoelastic behaviors of pullulan IL solutions are examined. It was observed that the behaviors change from Zimm like to Rouse like with increasing concentration, though the Zimm like behavior was not so apparent due to the higher tested concentration. The features of data are almost the same as typical ones observed for the ordinary dilute linear synthetic

polymer solutions. That is, in non-entangled regions of the solutions, the dynamic viscoelastic properties of pullulan ILs solutions coincide well with the calculation of Rouse-Zimm theory by using correction terms, which almost perfectly expressed the data for standard polystyrenes in good solvents. Concentration dependences of fitting parameters in the correction term, zero-shear viscosity η^0 and steady state compliance J_e obtained for pullulan in ILs solutions are also similar to those for the synthetic polymer in good solvents. By using M_w as floating parameter, it was pointed out that fitting the RZ model to the dynamic viscoelastic data can be used as a new characterization method to obtain M_w of insoluble natural polymers within ±30% error.

Publications

1. A study of density for pullulan/ionic liquids solutions.

Hu H, Takada A, and Takahashi Y.

Evergreen - Joint Journal of Novel Carbon Resource Sciences & Green Asia Strategy.

March (2014). 1(1), 14-19, 2014-03

2. Intrinsic viscosity of pullulan in ionic liquid solutions studied by rheometry.

Hu H, Takada A, and Takahashi Y.

Nihon Reoroji Gakkaishi (Journal of the Society of Rheology, Japan) 42(3), 191-196, 2014

3. Dynamic Viscoelastic Properties of Dilute Pullulan Ionic Liquids Solutions.

Hu H, Takada A, and Takahashi Y. Submitted.

Acknowledgment

First of all I am extremely grateful to my supervisor **Associate Prof. Yoshiaki Takahashi** for his instructive suggestions and valuable comments on this thesis. Without his invaluable help and generous encouragement I could not complete my thesis and graduate. He taught me a lot in professional knowledge and creative thoughts. At the same time I also want to thank **Assistant Prof. Akihiko Takada** for providing me with valuable advice and help on my thesis and daily life.

Thanks for all the students in this lab. It is very glad to stay with all of you during this six years. From them I learned a lot of different nation's culture and it will helpful for my career life in the future. I will miss the days we were together. At last, I want to thank my family for their support and endless love. My heart swells with gratitude to all the people who helped me.

Above all, please allow me to express my sincere thanks to all of you.